Global and Planetary Change 204 (2021) 103549

Contents lists available at ScienceDirect

Global and Planetary Change

journal homepage: www.elsevier.com/locate/gloplacha

Planktic foraminiferal changes in the western Mediterranean Anthropocene

Sven Pallacks [a,*], Patrizia Ziveri [a,b], Belen Martrat [c], P. Graham Mortyn [a,d], Michael Grelaud [a], Ralf Schiebel [e], Alessandro Incarbona [f], Jordi Garcia-Orellana [a,g], Griselda Anglada-Ortiz [a]

[a] Institute of Environmental Science and Technology (ICTA), Autonomous University of Barcelona (UAB), Bellaterra, Barcelona, Spain
[b] Catalan Institution for Research and Advanced Studies, Barcelona, Spain
[c] Department of Environmental Chemistry, Spanish Council for Scientific Research (CSIC), Institute of Environmental Assessment and Water Research (IDAEA), Barcelona, Spain
[d] Department of Geography, Autonomous University of Barcelona, Bellaterra, Barcelona, Spain
[e] Department of Climate Geochemistry, Max Planck Institute for Chemistry, Mainz, Germany
[f] Department of Earth and Marine Sciences, University of Palermo, Palermo, Italy
[g] Department of Physics, Autonomous University of Barcelona, Bellaterra, Barcelona, Spain

ARTICLE INFO

Editor: Dr. Fabienne Marret-Davies

Keywords:
Western Mediterranean Sea
Last 1500 years
Planktic foraminifera
Natural variability
Anthropogenic warming
Marine surface production

ABSTRACT

The increase in anthropogenic induced warming over the last two centuries is impacting marine environment. Planktic foraminifera are a globally distributed calcifying marine zooplankton responding sensitively to changes in sea surface temperatures and interacting with the food web structure. Here, we study two high resolution multicore records from two western Mediterranean Sea regions (Alboran and Balearic basins), areas highly affected by both natural climate change and anthropogenic warming. Cores cover the time interval from the Medieval Climate Anomaly to present. Reconstructed sea surface temperatures are in good agreement with other results, tracing temperature changes through the Common Era (CE) and show a clear warming emergence at about 1850 CE. Both cores show opposite abundance fluctuations of planktic foraminiferal species (*Globigerina bulloides*, *Globorotalia inflata* and *Globorotalia truncatulinoides)*, a common group of marine calcifying zooplankton. The relative abundance changes of *Globorotalia truncatulinoides* plus *Globorotalia inflata* describe the intensity of deep winter mixing in the Balearic basin. In the Alboran Sea, *Globigerina bulloides* and *Globorotalia inflata* instead respond to local upwelling dynamics. In the pre-industrial era, changes in planktic foraminiferal productivity and species composition can be explained mainly by the natural variability of the North Atlantic Oscillation, and, to a lesser extent, by the Atlantic Multidecadal Oscillation. In the industrial era, starting from about 1800 CE, this variability is affected by anthropogenic surface warming, leading to enhanced vertical stratification of the upper water column, and resulting in a decrease of surface productivity at both sites. We found that natural planktic foraminiferal population dynamics in the western Mediterranean is already altered by enhanced anthropogenic impact in the industrial era, suggesting that in this region natural cycles are being overprinted by human influences.

1. Introduction

Mankind's influence on the climate has grown over the last two centuries, with exponential enrichment of greenhouse gases in the atmosphere (Abram et al., 2016; Crutzen, 2002). As observed by comparing data retrieved from instrumental measurements and ice core records (Bauska et al., 2015; Friedli et al., 1986; Tans and Keeling, 2020), the unprecedented increase of atmospheric CO_2 accelerated during the 20th century, warming surface oceans (Gleckler et al., 2012) and depleting marine surface production through enhanced vertical stratification (Behrenfeld et al., 2006; Li et al., 2020). In a world subjected to high anthropogenic pressure and affected by a continuous increase in atmospheric CO_2 since the Industrial Revolution, knowledge about the impacts of rising sea surface temperatures (SST) on changes in marine productivity plays an important role in understanding biological and environmental changes in the ocean.

The Mediterranean Basin, as a climate change hotspot (Giorgi, 2006), is particularly affected by environmental changes. The western Mediterranean is under the influence of large scale atmospheric patterns like the North Atlantic Oscillation (NAO), since fluctuations of the

* Corresponding author.
E-mail address: sven.pallacks@uab.cat (S. Pallacks).

https://doi.org/10.1016/j.gloplacha.2021.103549
Received 21 January 2021; Received in revised form 22 May 2021; Accepted 15 June 2021
Available online 24 June 2021

atmospheric pressure gradient between the Icelandic Low and the Azores High are associated with changes in climatic and oceanographic conditions (Hurrell, 1995; Tsimplis et al., 2013; Ulbrich et al., 2012), altering marine ecosystems (Drinkwater et al., 2003). The Atlantic Multidecadal Oscillation (AMO) is closely linked to SST variations in the western Mediterranean Sea (Marullo et al., 2011). NAO and AMO varies on multidecadal to centennial time scales (Mann et al., 2009; Olsen et al., 2012; Trouet et al., 2009) with positive phases prevailing during the Medieval Climate Anomaly (MCA), a warm period which begins in the western Mediterranean at roughly 800 CE. With the onset of the Little Ice Age (LIA), a subsequent, cold period lasting from around 1300 CE to 1800 CE, negative NAO phases became predominant (Gray et al., 2004; Lüning et al., 2019; Moreno et al., 2012; J. Wang et al., 2017). The first part of the 20th century was characterized by low pressure gradients, whereas from the 1970s on, positive NAO phases were stronger and occurred more frequently (Hurrell, 2020). The high NAO index by the end of the 20th century appears unprecedented during the last 130 years (Osborn, 2004), but is not unusual in the context of the past centuries (Hernández et al., 2020). The close relation between NAO, AMO, and SST in the pre-industrial Mediterranean (Lüning et al., 2019) was superimposed by anthropogenic induced warming during the second half of the 20th century (Macías et al., 2013). Since 1880 CE, the annual mean air temperature has warmed more abruptly in the Mediterranean region compared to the global average (Cramer et al., 2018), accelerating the increase of SSTs in the Mediterranean at a rate of 0.35 °C per decade (Shaltout and Omstedt, 2014). Direct (changes in reproducibility, behavior, fitness and survival of marine organisms) and indirect (changes in biotic interactions or hydrography, e.g. displacement and intensity of marine currents, sea surface stratification) effects of ocean warming resulting in biogeographical shifts of species, mainly towards the northwest, causing a tropicalization and homogenization of the Mediterranean biota, and altering biodiversity and ecosystem functioning (Bianchi, 2007; Lejeusne et al., 2010; Philippart et al., 2011). Enhanced stratification as a consequence of sea surface warming is predicted to lower the primary production rate in the western basin, causing biomass loss in the entire Mediterranean Sea (Coma et al., 2009; Macías et al., 2015). Particularly calcifying organisms seem to be affected by climate-induced warming (Beaugrand et al., 2013).

The northwestern and southwestern Mediterranean regions are ideal locations to study impacts of natural versus anthropogenic climate change on surface ocean properties, since deep water formation in the Gulf of Lion is strongly connected to NAO variability (Josey et al., 2011; Vignudelli et al., 1999), driving surface productivity in the Alboran Sea (Macías et al., 2008; Macías et al., 2016; Macías et al., 2007). The see-saw pattern between high productive phases linked to strong deep water formation and vice versa is described in several Holocene marine sediment records (Ausín et al., 2015; Bazzicalupo et al., 2020; Cacho et al., 2000; Cisneros et al., 2019; Nieto-Moreno et al., 2015; Schirrmacher et al., 2019), while anthropogenic warming has affected both study regions, as reported through instrumental data and paleoenvironmental archives (Nieto-Moreno et al., 2013; Sicre et al., 2016).

Planktic foraminifera are single-celled marine eukaryotes producing calcite and yield an excellent marine sedimentary record. The sensitivity of planktic foraminifera to changing physical and chemical conditions and their good preservation in marine sediments makes them good tracers of changing environmental conditions, regardless of whether alterations are caused by natural or anthropogenic drivers. Planktic foraminifera are under the influence of several surface seawater properties (Bé, 1977; Bé and Tolderlund, 1971; Schiebel and Hemleben, 2017), although the most important factor controlling assemblage composition and diversity is SST (Jentzen et al., 2018; Morey et al., 2005; Rutherford et al., 1999). On a regional and seasonal scale, quality of food plays a crucial role for the distribution of surface to subsurface dwelling species (Schiebel et al., 2001), indicated by the close relation between marine primary production and flux rates of planktic foraminiferal tests (Kucera, 2007). Water column configuration and food availability are supposed to be the main factors controlling foraminiferal distribution, abundance and diversity in the Mediterranean Sea (Bárcena et al., 2004; Giamali et al., 2020; Pujol and Grazzini, 1995; Rigual-Hernández et al., 2012; Zarkogiannis et al., 2020), whereas differences in the seawater carbonate chemistry between the eastern and western basin play a minor role (Mallo et al., 2017). Post-industrial age changes in planktic foraminiferal assemblages in oceans are subtle, limited to ~ 600 km latitudinal shift compared to pre-industrial communities (Field et al., 2006; Jonkers et al., 2019; Schiebel et al., 2018). In the Mediterranean Sea, no evidence of anthropogenic influence on planktic foraminiferal assemblages has been documented. Even over the latest climate anomalies (e.g. MCA, LIA), the planktic foraminiferal response appears weak, with small percentage changes in selected species and/or in the ratio between taxa that indicate different local hydrographic conditions (Incarbona et al., 2019; Lirer et al., 2014; Margaritelli et al., 2018; Vallefuoco et al., 2012).

The main objectives of this study are to determine how natural climate change, in particular large scale atmospheric oscillations like the NAO and AMO, have driven planktic foraminiferal assemblage dynamics during the Common Era at two strategically ideal locations in the western Mediterranean to study high-frequency changes in water mass dynamics and marine surface productivity, and to assess if the signal of natural variability in planktic foraminiferal composition is superimposed by accelerated anthropogenic SST warming, starting with the onset of the Industrial Revolution. For this reason, we investigate the planktic foraminiferal accumulation rate records in two high resolution multicores collected in the Alboran Sea and the Balearic Sea spanning approximately the last 1.2 and 1.7 ky. We also report abundances of selected taxa in the > 150 μm fraction, to test the impact of large-scale atmospheric oscillations like the NAO and AMO during the Common Era. The planktic foraminiferal palaeoecological reconstruction is carried out along with data on alkenone-derived SST, organic biomarkers, and coccolithophore (calcifying phytoplankton) assemblage that provide evidence of a simultaneous modification in water column dynamics and in the planktic ecosystem network. Especially significant are $U^{k'}_{37}$ estimates that capture a pronounced post-industrial SST rise in both the Balearic and the Alboran seas, which is in line with instrumental measurements.

2. Study area

2.1. Oceanographic settings

The semi-enclosed Mediterranean Sea is separated by the Sicily Strait sill into the western and eastern Mediterranean basins. It is characterized by an anti-estuarine thermohaline circulation with eastward surface and westward subsurface flow, due to net buoyancy loss from west to east as a consequence of changes in evaporation, precipitation and runoff (Millot, 1999; Rohling et al., 2009; Schroeder et al., 2012; Schroeder et al., 2008). The Mediterranean Sea features large eastward surface gradients in physical and chemical characteristics with increasing salinity, SST, and alkalinity, and decreasing surface nutrient concentrations and dissolved inorganic carbon (Schneider et al., 2007; Shaltout and Omstedt, 2014; Stambler, 2014; Tanhua et al., 2013).

The two study sites, as shown in Fig. 1, are under the influence of large-scale atmospheric phenomena. The differences of atmospheric sea level pressure between the Icelandic Low and the Azores High, known as the NAO, is influencing the climate and oceanographic conditions of the western Mediterranean (Hurrell, 1995). Positive NAO phases characterized by a strong subtropical high-pressure cell and a deeper Icelandic Low generate strong westerly winds, crossing the Atlantic on a more northerly track and result in warm and dry conditions over the Mediterranean Sea with reduced storm activity and below average precipitation rates. A weak pressure gradient between the Azores High and the Icelandic Low (negative NAO phase) causes a more southeasterly pathway and enhanced storminess in southern Europe, which brings

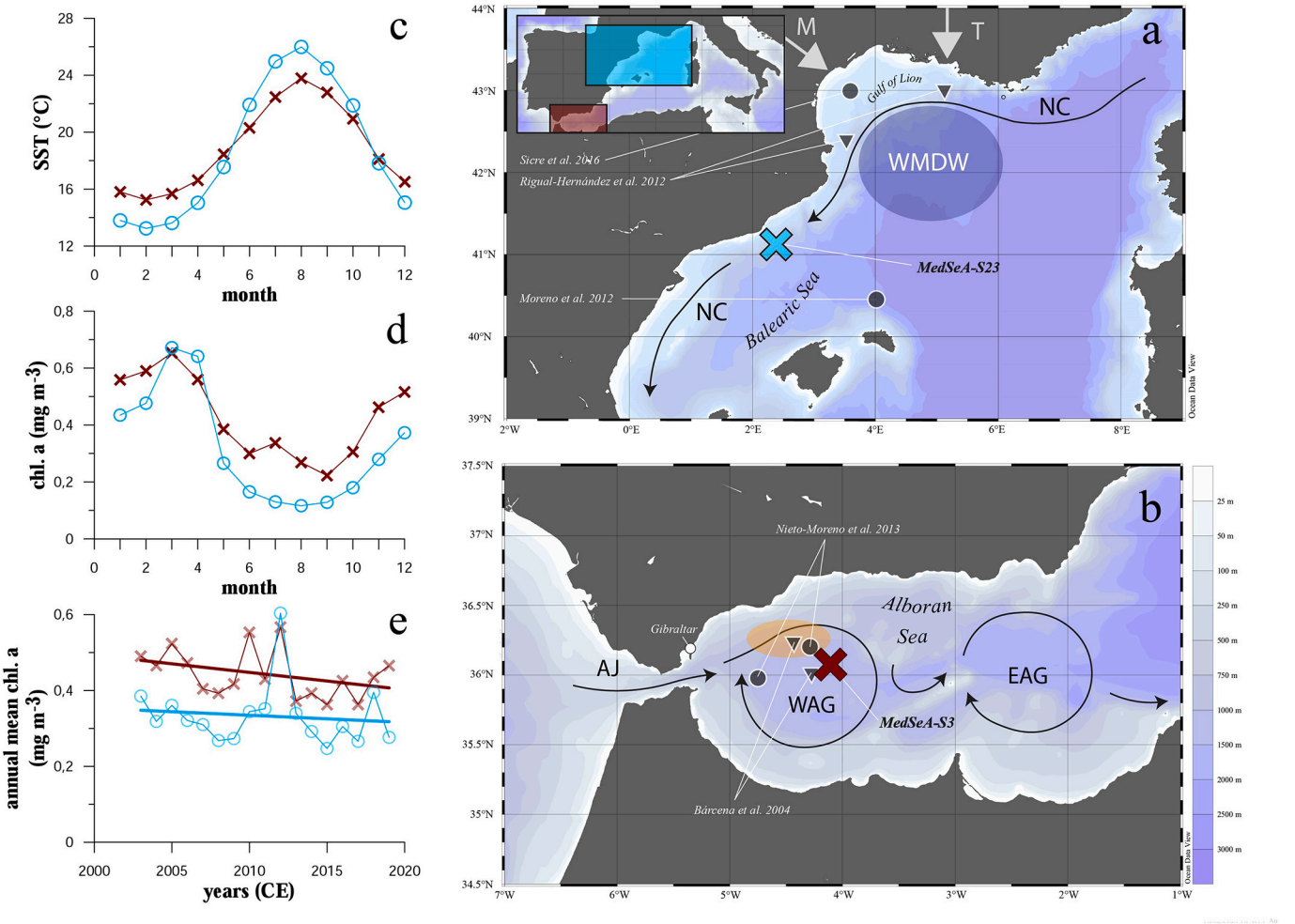

Fig. 1. Locations of the study areas in the western Mediterranean Sea, bathymetry, hydrography, SST, and chlorophyll-a data. (a-b) Ocean Data View (ODV) bathymetric maps (Schlitzer, 2019). Dark arrows represent surface currents and gyres. (a) Station MedSeA-S23 in the Balearic Sea. Core location indicated by a blue cross. NC: Northern Current (surface). WMDW: Western Mediterranean Deep Water formation. M: Mistral. T: Tramontana. (b) Station MedSeA-S3 in the Alboran Sea. Core location indicated by a red cross. AJ: Atlantic Jet (surface). WAG: Western Alboran Gyre. EAG: Eastern Alboran Gyre. Upwelling area (orange). References of studies close to core location cited in text. (c) Monthly sea surface temperature (SST), (d) Monthly surface chlorophyll-a concentration (e) annual mean chlorophyll-a concentration from 2003 to 2019 CE at the Balearic (blue open circles) and Alboran Sea (red crosses) core site. Linear fit for both time series indicated by blue (Balearic Sea) and red (Alboran Sea) line. Data is retrieved from AQUA-Modis, Level 3 sensor, covers the period from July 2002 to February 2020, and is centered at the exact core location, covering 16 km^2.

more moisture to the Mediterranean region (Ulbrich et al., 2012). NAO phases vary on annual to multicentennial time scales and are recorded in environmental archives like lake sediments, tree rings and speleothems, thus allowing for reconstructing high resolution records dating back several thousand years (Faust et al., 2016; Olsen et al., 2012; Smith et al., 2016; Trouet et al., 2009).

The AMO is a climate cycle varying on multidecadal to -centennial timescales, which affects SST of the North Atlantic Ocean. SST changes vary with an amplitude of 0.4 °C at their extremes on a 65–80 year cycle (Enfield et al., 2001; Schlesinger and Ramankutty, 1994). The AMO has a strong connection to SST changes in the western Mediterranean Sea. SSTs in the Mediterranean region exhibit a 70 year cyclicity, which is similar to the AMO variability, when looking at instrumental data (Marullo et al., 2011).

Each study site shows a characteristic hydrography, influenced by the previously described large-scale atmospheric patterns. As an end-member of the Mediterranean Atlantic Water (MAW) flowing through the Tyrrhenian Sea, the Northern Current (NC) connects the Gulf of Lion with the study area in the Balearic Sea (Millot, 1999). Primarily in the Gulf of Lion, Western Mediterranean Deep Water (WMDW) is formed through two oceanographic processes described as dense shelf water cascading and open-sea deep convection mainly in January to February due to cold air masses (Canals et al., 2006; Rohling et al., 2009). Cold, orographically channeled air from the northern European continent is causing strong evaporation and surface water cooling and results in buoyancy loss in the Gulf of Lion, thus affecting deep water formation (Medoc, 1970; Mertens and Schott, 1998; R. O. Smith et al., 2008). Interannual variabilities between cold and dry or warm and wet air masses have been detected and linked to the winter state of the NAO (Ausín et al., 2015; Cisneros et al., 2019; Josey et al., 2011; Vignudelli et al., 1999).

The hydrography of the Alboran Sea is mainly characterized by two anticyclonic, quasi-permanent gyres, the Western Alboran Gyre (WAG) and the Eastern Alboran Gyre (EAG) both spanning around 100 km in diameter (Gascard and Richez, 1985; Heburn and La Violette, 1990). Driven by the strength of the Atlantic Jet (AJ) (Bormans and Garrett, 1989; Flexas et al., 2006), the Alboran gyre system is characterized by a complex mesoscale variability and can vary between a one gyre (1G), two gyre (2G) or three gyre (3G) system (Peliz et al., 2013; Renault et al., 2012; Vargas-Yáñez et al., 2002). Variations in the Mediterranean Thermohaline Circulation (MTHC) during winter months force surface net water flux into the Mediterranean Sea through the Strait of Gibraltar

(SoG), to compensate for water masses transported to the interior during deep water formation. The MTHC is the main mechanism controlling velocity and direction of the AJ, whereas local wind forcing and sea level pressure are playing a minor role (Macías et al., 2016). Upwelling in the region is controlled by winds and direction and velocity of the AJ (Macías et al., 2008; Macías et al., 2007; Sarhan et al., 2000). A strong AJ located northwards along the Spanish coast and prevailing westerlies cause coastal upwelling and result in highly fertile, nutrient rich surface water. Weak Atlantic water inflow and presence of easterlies induces a southward shift of the AJ, moving the upwelling area further offshore and generating less fertile surface water conditions in the northwestern Alboran region (Fig. 1b).

2.2. SST and surface productivity at the two study sites

Satellite-derived data from 2003 to 2019 (AQUA-Modis, Level 3) shows with 18.8 °C (Balearic Sea) and 18.9 °C (Alboran Sea) an almost equal mean annual SST at both study sites, whereas higher mean annual chlorophyll-a concentrations of 0.44 mg m^{-3} at the Alboran core station, compared to 0.33 mg m^{-3} in the Balearic Sea site, confirm the Alboran Sea to be a high productivity area (NASA Goddard Space Flight Center, Ocean Ecology Laboratory, Ocean Biology Processing Group, 2020). The Balearic Sea is characterized by lower productivity levels compared to the Alboran Sea, but is still one of the high productivity regions in the Mediterranean Sea (Colella et al., 2003; Stambler, 2014). As shown in Fig. 1c, seasonal SST variations in the Balearic Sea (August: 26.0 °C; February: 13.2 °C) have a higher amplitude compared to the Alboran Sea (August: 23.7 °C; February: 15.2 °C). In the Balearic Sea, SSTs are mainly controlled by warm summer and cold winter airflow, coming from the European continent, whereas cold Atlantic water inflow influences SST at the Alboran study site.

With highest productivity in March (0.64 mg m^{-3}) and lowest values in August (0.12 mg m^{-3}), primary production is driven by the annual cycle of the thermal structure of the water column in the northwestern Mediterranean. High summer SSTs cause a strong stratification of the water column, impeding vertical advection of nutrients to the surface causing oligotrophic conditions. Cold katabatic winds during winter enhance deep mixing and surface nutrient supply, which leads to high primary production by late winter to early spring, amplified by higher solar radiation. Interannual variabilities between cold and dry or warm and wet air masses influencing the deep water formation in the Gulf of Lion through buoyancy loss, have been detected and linked to the winter state of the NAO (Cisneros et al., 2019; Josey et al., 2011; Vignudelli et al., 1999). At the Alboran core station, highest chlorophyll-a concentrations occur in March (0.66 mg m^{-3}) and lowest ones in August (0.22 mg m^{-3}). High primary productivity levels are the consequence of fresh nutrient rich upwelled water at the northern Alboran Sea (Bárcena and Abrantes, 1998; Bárcena et al., 2004; Garcia-Gorriz and Carr, 2001), the local occurrence of which is highly dependent on the hydrography of the WAG system.

3. Material and methods

3.1. Material

The study is based on high resolution multicore records (MedSeA-S3-c1; MedSeA-S23-c1; MedSeA-S23-c3), collected at two sites of the western Mediterranean Sea with a MC400-Multicorer system during the MedSeA cruise (Mediterranean Sea Acidification in a changing climate) on 2 May to 2 June 2013 onboard the R/V Àngeles Alvariño. Core MedSeA-S3-c1 was retrieved in the Alboran basin (Lat. 36.0746° N, Long. 04.11040° W) at a water depth of 1137 m, with a core length of 33 cm. Cores MedSeA-S23-c1 and MedSeA-S23-c3 were recovered at a water depth of 1156 m in the Balearic basin offshore Barcelona (Lat. 41.1121° N, Long. 2.38200° E) with core lengths of 43 cm. MedSeA-S23-c3 was sliced onboard every cm, whereas MedSeA-S23-c1 was processed after the cruise and sliced every 0.5 cm.

3.2. Radiocarbon and radionuclides analysis

Determination of total ^{210}Pb activities was accomplished through the measurement of its alpha-emitter daughter nuclide ^{210}Po, following the methodology described in Sánchez-Cabeza et al. (1998) at the Autonomous University of Barcelona. After addition of ^{209}Po as an internal tracer, sample aliquots of 200–300 mg were totally digested in acid media by using an analytical microwave oven and Po isotopes plated on silver discs in HCl 1N at 70 °C while stirring for 8 h. Po emissions were subsequently counted using α-spectrometers equipped with low-background silicon surface barrier (SSB) detectors (EG&G Ortec) for $4x10^5$ seconds. The concentrations of excess ^{210}Pb used to obtain the age models were determined as the difference between total ^{210}Pb and the uniform ^{210}Pb at depth. Maximum mean sediment accumulation rates and therefore the age-depth model over the last decades/century was estimated using the Constant Flux : Constant Sedimentation (CF:CS) model (Krishnaswamy et al., 1971; Robbins, 1978).

Radiocarbon dating (^{14}C) was performed on the lower part of cores MedSeA-S3-c1 and MedSeA-S23-c1. Planktic foraminifera (*Globorotalia inflata*) isolated from the 250 – 315 μm fraction from two different depths (MedSeA-S3-c1: 15–16 cm, 30–31 cm and MedSeA-S23-c1: 19.0–19.5cm, 39.0–39.5 cm) were used for radiocarbon dating. Analysis was performed by using accelerator mass spectrometry (AMS) at the NOSAMS facility at Woods Hole Oceanographic Institution (Volkman et al., 1995). Taking the marine radiocarbon reservoir effect into account, with an offset of 400 years (Siani et al., 2000), radiocarbon ages were calibrated to calendar ages by using Marine13 calibration curve (Reimer et al., 2013) where ages were reported with a 2σ uncertainty. The age-depth models of the sediment records were obtained by combining the surficial age models obtained from the ^{210}Pb activity-depth profiles with the ages obtained using the ^{14}C technique from planktic foraminifera from sections 15.5 cm to 30.5 cm (MedSeA-S3-c1) and 19.25 cm to 39.25 cm (MedSeA-S23-c1) (Appleby and Oldfield, 1992; Bradley, 2015).

The age-depth models for the entire sediment cores in the Alboran and the Balearic Seas were calculated considering both ^{14}C dates and the ages from the 20th century reported by the ^{210}Pb age model (up to 5.5 cm core depth of MedSeA-S3-c1, up to 11.5 cm core depth of MedSeA-S23-c1 and MedSeA-S23-c3) and using Bayesian statistics applied by the R-code package "rbacon" (Blaauw and Christen, 2011) shown in Figs. S1, S3 and S4.

3.3. Biomarkers

Alkenones (heptatriaconta-8E,15E,22E-trie2-one and heptatriac onta-15E,22E-die2-one) of core MedSeA-S3-c1 and MedSeA-S23-c3 were extracted from sediments, purified using organic solvents and quantified with a Varian gas chromatograph Model 450 equipped with a septum programmable injector, flame ionization detector and a CPSIL-5 CB column (coated with 100% dimethyl siloxane; film thickness of 0.12 μm; L(m) * ID(mm) * OD(mm): 50 * 0.32 * 0.45). Hydrogen was the carrier gas (2.5 mL min^{-1}). Concentrations were determined using n-hexatriacontane ($CH_3(CH_2)_{34}CH_3$) as an internal standard. Absolute concentration errors were below 10% (resolution between the alkenones from 1.5 to 1.7). Reproducibility tests showed that uncertainty in the $U^{k'}_{37}$ determinations was lower than 0.015 (ca. 0.5 °C) (Cacho et al., 1999; Martrat et al., 2004; Martrat et al., 2014; this study), confirming the precision of this paleothermometry tool (Eglinton et al., 2001). SST reconstructions are based on the global calibration of Conte et al. (2006), estimating the standard error on surface sediments at 1.1 °C.

3.4. Planktic foraminifera

3.4.1. Taxonomic concepts

Analysis of planktic foraminiferal tests was performed on cores MedSeA-S3-c1 and MedSeA-S23-c1. The five morphospecies *Globigerinoides ruber* (d'Orbigny 1839), *Globigerina bulloides* (d'Orbigny 1826), *Globorotalia inflata* (d'Orbigny 1839), *Globorotalia truncatulinoides* (d'Orbigny 1839), and *Orbulina universa* (d'Orbigny 1839) were isolated. Classification of the different foraminiferal species was carried out by visual identification using a binocular stereo microscope (magnification 10× - 20×) and a bifurcated illuminator. Taxonomic identification of the target species was based on Schiebel and Hemleben (2017). The white (*G. ruber*$_{WHITE}$) and pink (*G. ruber*$_{PINK}$) varieties were collected separately. A distinction between the two morphotypes of *G. ruber*$_{WHITE}$, *G. ruber* sensu lato (*G. ruber*$_{SL}$) and *G. ruber* sensu stricto (*G. ruber*$_{SS}$) was made, based on differences in test morphology (Kontakiotis et al., 2017; Numberger et al., 2009; L. Wang, 2000)

3.4.2. Analyzed size fraction

Bulk sediment mass was obtained after drying samples at 60 °C for approximately 24 hours. Samples were washed over a 63 μm screen using distilled Elix water. The size fraction larger than 63 μm was oven dried at 60 °C for 1 - 2 hours. Samples were dry sieved and divided by a Riffle Splitter at the chosen size fractions, 150–250, 250–315 and > 315 μm. Results are presented and discussed for > 150 μm size fraction. More than 300 specimens were identified in the > 150 μm size fraction in all samples.

The standard > 150 μm analysis for planktic foraminifera analysis in the oceans is a legacy of the CLIMAP project (CLIMAP Project Members et al., 1984), mainly aimed at reconstructing SST variations in the oceans over glacial-interglacial cycles and benefits from a huge modern reference database (Schmidt et al., 2004). This fraction is commonly used by Mediterranean specialists even if some species would be underrepresented, among others *Turborotalita quinqueloba*, an important proxy for surface productivity during glacials (Capotondi et al., 2004; Di Donato et al., 2015; Sprovieri et al., 2003). The number of total planktic foraminiferal shells and their total accumulation rate was evaluated on the > 150 μm size fraction.

3.5. Coccolithophore sedimentary record

Analysis of relative abundance of calcareous nannoplankton assemblages (coccolithophores) was done on core MedSeA-S3-c1. Following standard procedures in Bown and Young (1998) smear slides of each sample (<63 μm) were prepared and analyzed by a polarized microscope (x 1000 magnification). Considering around 20 taxonomic units, at least 500 specimens were counted and identified by taxonomic concepts of extant coccolithophores (Young et al., 2003).

4. Results

4.1. Age model

Concentrations of $^{210}Pb_{tot}$ and $^{210}Pb_{xs}$ with depth in the sediment records are shown in Figs. S1, S3 and S4. $^{210}Pb_{tot}$ activity of the 3 analyzed cores is decreasing from the surface, reaching a constant average value ($^{210}Pb_{sup}$) of ~31 ± 2 Bq kg^{-1} at ~12.5 cm depth (MedSeA-S3-c1), ~35 ± 3 Bq kg^{-1} at ~20.5 cm depth (MedSeA-S23-c1) and ~33 ± 2 Bq kg^{-1} at ~18.5cm depth (MedSeA-S23-c3). Applying the CF:CS model the maximum mean mass accumulation rate (MAR) is 0.047 ± 0.002 g cm^{-2} yr^{-1} (MedSeA-S3-c1), 0.105 ± 0.008 g cm^{-2} yr^{-1} (MedSeA-S23-c1), and 0.110 ± 0.004 g cm^{-2} yr^{-1} (MedSeA-S23-c3). Combining the calculated ^{210}Pb ages for the upper core parts (first 5.5 cm and 11.5 cm for cores MedSeA-S3-c1 and MedSeA-S23-c1, respectively) with calibrated ^{14}C ages at depth 15.5 cm (1297 yr CE, 2σ cal 1257 – 1337 yr CE) and 30.5 cm (433 yr CE, 2σ cal 358 – 534 yr CE) of core MedSeA-S3-c1, and at depth 19.25 cm (1481 yr CE, 2σ cal 1442 – 1529 yr CE) and 39.25 cm (1050 yr CE, 2σ cal 992 – 1140 yr CE) of core MedSeA-S23-c1, through Bayesian modelling approach, an age depth model was calculated. The mean sedimentation rate (SR) is 33.5 cm kyr^{-1} (MedSeA-S3-c1), 50.6 cm kyr^{-1} (MedSeA-S23-c1), and 53.8 cm kyr^{-1} (MedSeA-S23-c3) (Table S1).

4.2. Absolute changes in reconstructed SST

Data on SST and alkenone concentration of both records is summarized in Fig. 2 and Data Set S4 & S5 (Supplementary Information). In the Balearic Sea record, SST ranged between 16.0 °C to 18.0 °C, with slightly higher SST during the MCA (17.0 °C; 895 – 1135 CE) than during the LIA (16.8 °C; 1135–1755 CE). An SST drop to ~16.2 °C is detected between 1135 CE and 1195 CE, and to 16.0 °C around 1851 CE. The 20th century is marked by an SST increase of almost 2 °C. SST recorded in the Alboran Sea is ranging between 18.8 °C and 17.3 °C. Differences between MCA (18.4 °C; 378 – 1046 CE) and LIA (17.7 °C; 1103 – 1762 CE) are more pronounced than in the Balearic Sea. Two minimums of SST are detected at the end of the 13th century (17.3 °C) and at the end of the 1960s CE (17.4 °C). An SST warming is detected from the 1970s of up to 18.6 °C.

4.3. Planktic foraminiferal species abundances

Even though the time interval under investigation is comparably short, assuming little changes in climatological and oceanographic conditions, some species reveal large abundance variations and trends at both study sites, beyond the 95% confidence level errors related with counting (Fig. 3, Data Set S1 & S2).

In the Balearic Sea record, *G. bulloides* is the dominant target species (5.4–26.2%, on average 17.6%) followed by *G. truncatulinoides* (2.3–12.7%, on average 6.7%), *G. inflata* (1.6–10.8%, on average 4.6%) and *G. ruber*$_{WHITE}$ (0.2–8.6%, on average 3.6%). The Alboran Sea record reveals *G. bulloides* (28.0–57.4%, on average 38.2%) and *G. inflata* (17.6–44.9%, on average 27.5%) as the two dominant species, followed by *G. ruber*$_{WHITE}$ (4.8–11.5%, on average 7.9%). In both Balearic and Alboran records, the morphospecies *G. ruber*$_{SL}$ (0.1–8.0% and 3.6–9.1%, on average 3.2% and 5.9%, respectively), which occurs mainly as "platys" and elongate morphotypes, dominates over *G. ruber*$_{SS}$ (0–2.1% and 0.6–3.7%, on average 0.4% and 2.0%, respectively). Other selected species are less abundant on average (< 2%). Noteworthy, *G. bulloides*, *G. inflata* and *G. truncatulinoides* show abundance fluctuations of opposite signs at their core locations over some time intervals, but also between study sites (Fig. 3). Due to their low relative abundances, variations in *G. ruber*$_{SS}$, *G. ruber*$_{PINK}$ and *O. universa* are not statistically significant. Only the morphospecies *G. ruber*$_{SL}$ displays significant abundance changes in both records at the Balearic Sea site during the Common Era.

To display modern planktic foraminiferal productivity during the last 30 years, the annual mean test accumulation rates for core top samples representing the time period between 1980 to 2013 CE were calculated, showing higher rates in the Alboran (30.1 ind. cm^{-2} yr^{-1}) than in the Balearic (22.5 ind. cm^{-2} yr^{-1}) record. In both cores, the gradual increase of test accumulation rates occurs within radionuclide dating. The rates of test flux per gram of sediment and the standardized test accumulation rates show accelerated declines during the 20th century at both study areas.

4.4. Calcareous nannoplankton species composition

Calcareous nannofossils are well preserved, indicating absence of significant dissolution phenomena. The entire assemblage of counted and identified species is available in Data Set S3 (Supplementary Information). Taxa do not show any significant abundance variation throughout the record, except for *Emiliania huxleyi*, *Gephyrocapsa oceanica* and *Florisphaera profunda* since the 20th century (Fig. 2). Most

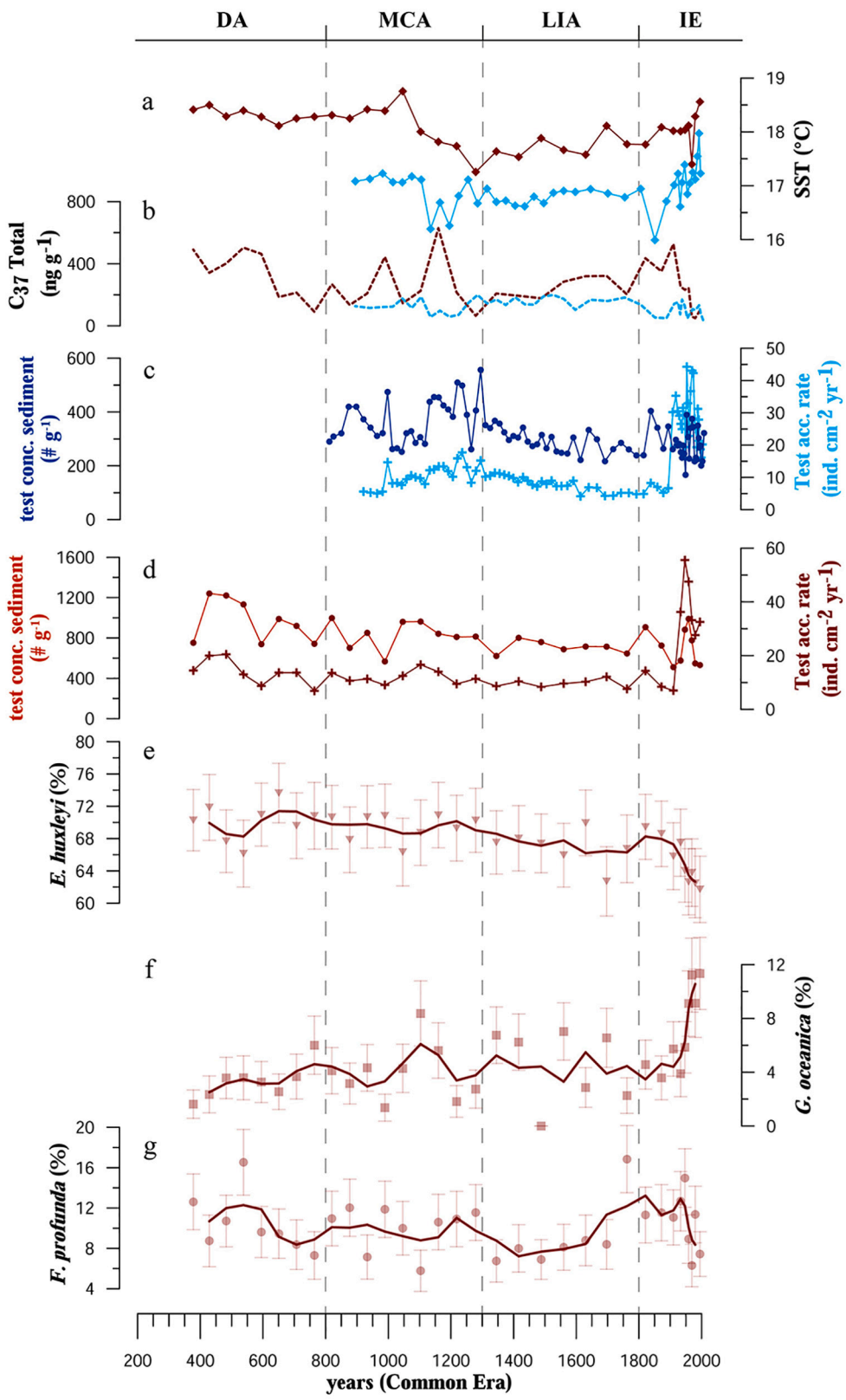

Fig. 2. Downcore variations of SST, surface production of calcareous organisms and relative abundances of calcareous nannoplankton taxa during the Common Era in the Alboran (red) and Balearic cores (blue). (a) Alkenone ($U^{k'}_{37}$) derived SSTs. (b) Alkenone concentration of total C_{37}. (c-d) Test accumulation rates and test concentrations per gram sediment in Balearic and Alboran cores. (e-g) Red symbols show percentage values of calcareous nannoplankton species, with 95% confidence interval of the counts indicated by the error bars. Red lines show 3-pt running average of calcareous nannoplankton species data. Duration of the Dark Age (DA), Medieval Climate Anomaly (MCA), Little Ice Age (LIA) and Industrial Era (IE) is based on estimates by Nieto-Moreno et al. (2011).

strikingly, relative abundances of *G. oceanica* triple over the past 100 years in the Alboran core and *E. huxleyi* and *F. profunda* show a continuous and gradual decrease.

5. Discussion

5.1. Age model

Age depth-models calculated for both study sites are in good agreement with results from other studies obtained nearby (Cisneros et al.,

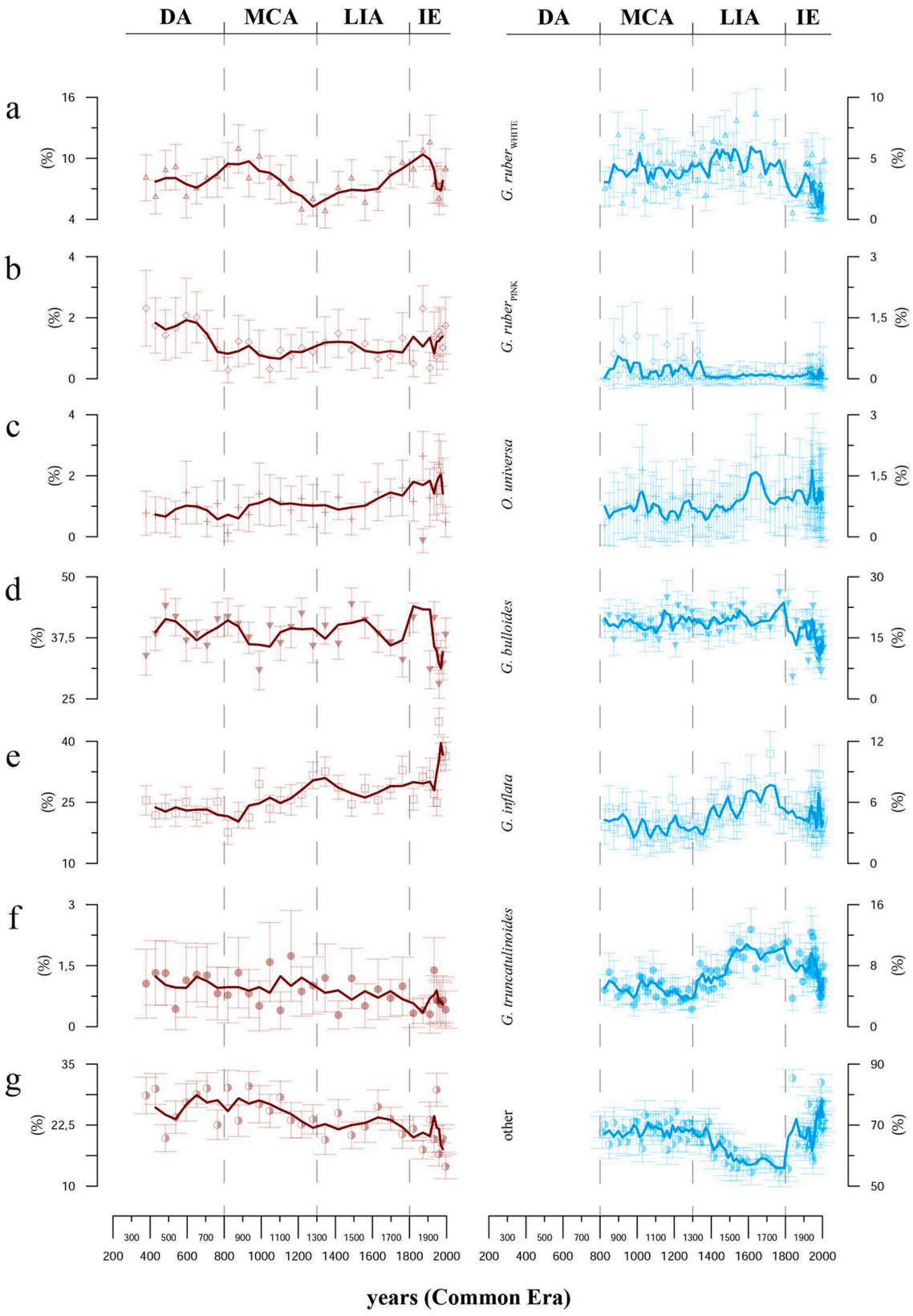

Fig. 3. Downcore variations of relative planktic foraminiferal species abundances (a-g) during the Common Era in the Alboran (red) and Balearic cores (blue). Symbols show percentage values of planktic foraminiferal species with 95% confidence interval of the counts indicated by the error bars. Solid lines indicate 3-pt running average of >150 μm size fraction of planktic foraminiferal species. Duration of the Dark Age (DA), Medieval Climate Anomaly (MCA), Little Ice Age (LIA) and Industrial Era (IE) is based on estimates by Nieto-Moreno et al. (2011).

2016; Frigola et al., 2007; Masqué et al., 2003; Moreno et al., 2012; Puig et al., 2015), further discussed in the Supplementary Information (Text S2). There is a rapid change in sedimentation rate from the upper (oldest ^{210}Pb date; MedSeA-S3-c1: 1925 ±4 yr CE at 5.5 cm core depth; MedSeA-S23-c1: 1922 −8 +7 yr CE at 11.5 cm; MedSeA-S23-c3: 1926 ±7 yr CE at 11.5 cm) to the lower core section (youngest ^{14}C date; MedSeA-S3-c1: 1297 −45 +40 yr CE at 15.50 cm core depth; MedSeA-S23-c1: 1481 −39 +48 yr CE at 19.25 cm), which we attribute to changes in sediment consolidation. Due to higher overburden, deeper parts of the core experience a higher consolidation leading to lower sedimentation rates, whereas unconsolidated top core sediments have a very high sedimentation rate. Due to the lack of a high-resolution age control, sedimentation rate changes because of poor consolidation are detected by abrupt changes in our age models. Rapid changes in sedimentation rates between core parts based on high resolution ^{210}Pb dates and low resolution ^{14}C dating are also reported in other studies (Cisneros et al., 2016; Margaritelli et al., 2020a). By increasing the numbers of ^{14}C datings below the unconsolidated core part, the distortion would be partly removed, as can be seen in the study of Sicre et al. (2016). Abrupt changes in sedimentation rates may be influenced by uncertainties when measuring ^{14}C and ^{210}Pb activity, like differences in reservoir ages in seawater (Alves et al., 2018; Ascough et al., 2005; Philippsen, 2013; Siani et al., 2000; Struglia et al., 2004), carbonate tests (Barker et al., 2007; Waelbroeck et al., 2001) or vertical lead diffusion and mixing (Mekik, 2014; Nittrouer et al., 1984), which is further discussed in Supplementary Information (Text S2).

The poor detection of changing sedimentation rates due to sediment consolidation behavior and the uncertainties occurring when combining ^{210}Pb and ^{14}C dating techniques, are both influencing parameters which are dependent on sedimentation rate. As a result, test accumulation rates seem to be overestimated in the upper (dataset based on ^{210}Pb dating) and underestimated in the lower core part (dataset based on ^{14}C dating), causing an anomalous increase at the beginning of the 20th century (Fig. 2). Through standardization of both datasets, setting variation on the same scale, not the amplitude of varying test accumulation rates, but the slope between the two datasets becomes comparable. Despite the above mentioned difficulties when combining age models derived from ^{210}Pb and ^{14}C dating results, to obtain high resolution age control, we reconstructed a robust age-depth model, supported by changing parameters independent from sedimentation rate, like relative abundance

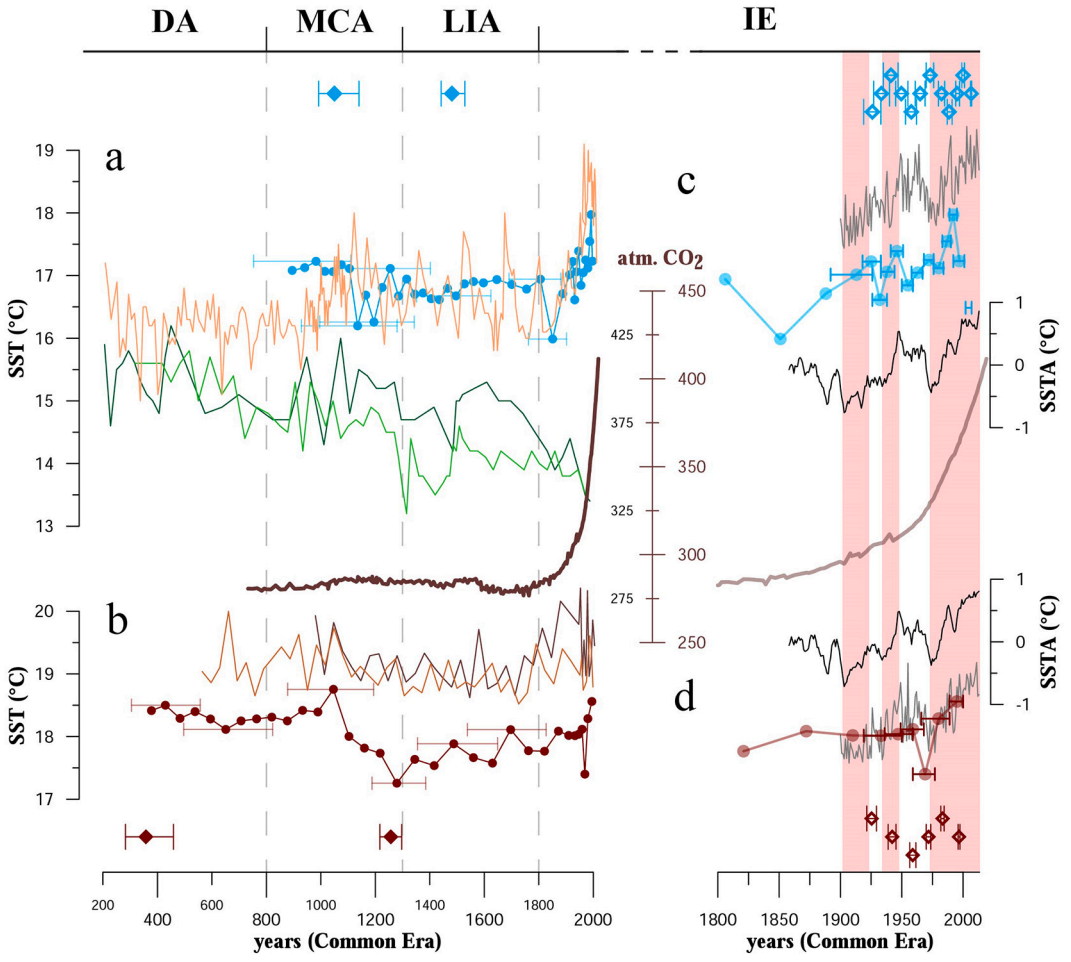

Fig. 4. SST records from the Balearic and Alboran Seas in comparison with nearby paleorecords and instrumental measurements with a focus on the Industrial Era. (a) Alkenone derived SST in Balearic core (blue circles). Paleotemperature records of other studies conducted in vicinity of the Balearic study site: light and dark green lines (Moreno et al., 2012); orange line (Sicre et al., 2016). (b) Alkenone derived SST in Alboran core (red circles). Paleotemperature records of other studies conducted in vicinity of the Alboran study site: light and dark brown (Nieto-Moreno et al., 2013). Industrial SST warming at the Balearic (c) and the Alboran (d) study site. Annual SST and standardized SST anomaly (SSTA), respectively, obtained through instrumental data: grey line (HadISST) and dark line (Kaplan v2) (Kaplan et al., 1998; Rayner et al., 2003; Reynolds and Smith, 1994). Red bands indicate SST warming phases derived from Kaplan and HadISST data. Blue and red circles, respectively, show alkenone derived SST in Balearic and Alboran core. Brown line shows atmospheric CO_2 concentrations measured (Tans and Keeling, 2020) and reconstructed (Friedli et al., 1986). Filled and open diamonds represent ^{14}C dates and ^{210}Pb dates used as tie-points for age-depth model reconstruction, respectively, color coded by the corresponding core color (Alboran = red; Balearic = blue), including their associated 2σ errors. Duration of the Dark Age (DA), Medieval Climate Anomaly (MCA), Little Ice Age (LIA) and Industrial Era (IE) is based on estimates by (Nieto-Moreno et al., 2011).

of principal planktic foraminiferal species (see 5.3.3), and alkenone-derived SST (see 5.2), which coincide with main environmental changes recorded independently.

5.2. SST changes over the past 1600 years

$U^{k'}_{37}$ SST estimates show good accordance in comparison to instrumental measurements (HadISST & Kaplan SST V2 data) and paleorecords (Fig. 4). With values ranging between 16–18 °C at the Balearic and 17–19 °C at the Alboran core site, they are generally consistent with other late Holocene $U^{k'}_{37}$ SST estimates (Cacho et al., 1999; Martrat et al., 2014; Schirrmacher et al., 2019; Sicre et al., 2016), displaying modern annual mean temperature differences at the study regions (Fig. 1c). Lower paleotemperatures (14–16 °C) estimated by Moreno et al. (2012) for the northwestern Mediterranean, can be explained by effects on the sedimentary alkenone signal through variability in surface production and/or differential degradation of 37:3 and 37:2 alkenones. When corrected, as done by Sicre et al. (2016) using the temperature calibration of Conte et al. (2006), SSTs coincide with estimates from our study. Alboran SST estimates are slightly lower compared to values (18.5–20 °C) obtained by Nieto-Moreno et al. (2013), but are still inside the lower range for autumn and average annual SSTs in the Alboran basin during the Holocene (Cacho et al., 1999; Pérez-Folgado et al., 2003). The core location in the Alboran Sea has a strong Atlantic influence, whereas the study area in the Balearic Sea is in close vicinity to the deep-water mass formation area, known for strong winter convection (Rohling et al., 2009; Skliris et al., 2012). Even though both areas are influenced by different meteorological and oceanographic conditions, they display similar SST trends. This suggests that both study sites are under the influence of larger-scale processes.

The prolonged pre-industrial cooling trend throughout the MCA and LIA is consistent with regional (Europe, Mediterranean Sea, and North Atlantic Ocean) and global ocean cooling from 0 CE to 1800 CE (McGregor et al., 2015). The sedimentary records reported here are in phase with climatic oscillations during the past millennium describing warmer SSTs during the MCA compared to the LIA (Lüning et al., 2019; Mann et al., 2009). Taking into account age error uncertainties, both records describe a ~ 1.0 °C cooling during the MCA-LIA transition between 1100 to 1300 CE, synchronous with the 1257 CE eruption event (Crowley and Unterman, 2013), which is associated with the onset of the LIA. The marked temperature drop below 16 °C at the Balearic core site at approximately 1851 −89 +51 yr CE could be related to the 1809 CE 'unknown' and the 1815 CE Tambora volcanic eruptions, as recorded in northeastern Mediterranean marine records (Gogou et al., 2016), marking the terminal point for the long-term cooling trend during the pre-industrial Common Era, followed by warming in the last two centuries.

With increasing SSTs starting in the 19th century, and accelerated sea surface warming during the 20th century, both cores display the temperature signal, already recorded in the Balearic (Sicre et al., 2016) and Alboran Sea (Nieto-Moreno et al., 2013), affirming pronounced 20th century warming in the western Mediterranean Sea (Lionello et al., 2006; Skliris et al., 2012; Vargas-Yáñez et al., 2010). The absence of a 20th century warming signal in cores collected at the Minorca contourite (Moreno et al., 2012) can be ascribed to a lack of age control over the past 500 years and age model extrapolation in the upper core part. Fig. 4 shows in detail SST reconstruction in the Balearic and Alboran Sea, compared to instrumental annual mean data estimated at core locations retrieved from temperature time series average over a 5° × 5° grid from Kaplan SST V2 data and the Hadley Centre Sea Ice and Sea Surface Temperature data set (HadISST) (Kaplan et al., 1998; Rayner et al., 2003; Reynolds and Smith, 1994). Industrial SST warming starting around 1850 CE is well captured by both instrumental and proxy data, describing the two phase warming of the western Mediterranean (Lionello et al., 2006), and importantly the exact moment of warming emergence under anthropogenic pressure in most of sites globally (Abram et al., 2016). SST rise during the last two centuries is more pronounced in the Balearic (2.0 °C) than in the Alboran record (0.8 °C), accelerating during the 20th century with an SST increase of more than 1°C at both study sites. This is in good agreement with satellite-derived mean annual warming rate of 0.026 °C yr^{-1} for the western Mediterranean basin during that period (Skliris et al., 2012).

5.3. Planktic foraminifera

5.3.1. Total planktic foraminiferal production

Modern mean test accumulation rates are calculated for 1980 CE to 2013 CE to provide an average value for planktic foraminiferal productivity and to make our results comparable to previous studies conducted during the last 30 years (Bárcena et al., 2004; Mallo et al., 2017; Pujol and Grazzini, 1995; Rigual-Hernández et al., 2012). Modern mean test accumulation rates are higher at the Alboran (30.1 ind. cm^{-2} yr^{-1}) than in the Balearic (22.5 ind. cm^{-2} yr^{-1}) core site. Our findings are in accordance with results from sediment traps, deployed at water depths between 1000 and 2000 m showing that 28.6 to 35.5 ind. cm^{-2} yr^{-1} in the western Alboran Sea (Bárcena et al., 2004; Hernández-Almeida et al., 2011) and 8.2 to 15.0 ind. cm^{-2} yr^{-1} in the northwestern Mediterranean Sea (Rigual-Hernández et al., 2012), displaying different trophic conditions at the two study sites. Due to nutrient rich upwelling at the northern edge of the WAG (Fig. 1b), the Alboran Sea is one of the most productive marine regions in the Mediterranean (Garcia-Gorriz and Carr, 2001). The Balearic Sea is characterized by lower productivity, even if the highly dynamic character of the region with strong frontal activity (La Violette, 1990) still makes it a more productive region in the rather oligotrophic Mediterranean Sea (Stambler, 2014). Annual average chlorophyll-a values (Fig. 1e) derived from satellite images during the last decades show higher values in the Alboran than in the Balearic study area and support the hypothesis of a positive correlation between primary production and planktic foraminiferal standing stocks, as phytoplankton serve planktic foraminifera as a major food source (Hemleben et al., 1989; Schiebel and Hemleben, 2005).

Foraminiferal accumulation rates in the core top samples of our study were comparable to the export fluxes estimated in sediment traps (Bárcena et al., 2004; Rigual-Hernández et al., 2012) from the western Mediterranean, supporting high consistency from sinking to accumulation in the sediment bed. In addition, the high carbonate saturation horizon throughout the water column in the Mediterranean Sea, suggest carbonate dissolution being unlikely (Millero et al., 1979; Schneider et al., 2007).

5.3.2. Planktic foraminiferal assemblage composition

Planktic foraminiferal core top assemblages in the Balearic and Alboran Sea are in good agreement with recent sediment trap, plankton tow, and core top studies conducted nearby (Bárcena et al., 2004; Hernández-Almeida et al., 2011; Mallo et al., 2017; Pujol and Grazzini, 1995; Rigual-Hernández et al., 2012; Thunell, 1978). In the northwestern Mediterranean, *G. ruber*$_{WHITE}$ (including the two morphotypes), *G. ruber*$_{PINK}$ and *O. universa* are part of the summer assemblage associated with low surface productivity. *Globigerina bulloides*, *G. truncatulinoides,* and *G. inflata* are dominant from winter to spring, when cold temperatures driving winter-deep mixing and causing high surface chlorophyll-a concentrations, which stimulate planktic foraminiferal productivity and cause high export fluxes and high accumulation rates to the seafloor sediment (Rigual-Hernández et al., 2012). In the western Alboran Sea, *G. bulloides* is the dominant species during periods of high productivity in spring and fall, whereas *G. inflata* has highest relative abundances during winter and summer, characterized by stratification of the water column, reduced upwelling and less productive conditions (Bárcena et al., 2004; Kontakiotis et al., 2016).

The species composition is assumed to reflect the climatic and oceanographic differences at both study sites. *Globigerinoides ruber*$_{WHITE}$ is a surface dwelling, symbiont bearing warm water species (Bé and

Tolderlund, 1971; Schiebel et al., 2002). Although it is a shallow dwelling species, it may occur at nutricline depths in less turbid oligotrophic waters (Pujol and Grazzini, 1995; Schiebel et al., 2004; Zarkogiannis et al., 2020). *Globigerinoides ruber*$_{PINK}$ seems to exhibit high sensitivity to changing SST, and to prosper only at maximum SSTs (Mallo et al., 2017). *Orbulina universa* has a high tolerance to temperature and salinity (Anderson et al., 1979; Bijma et al., 1990). As a symbiont bearing species, *O. universa* is restricted to the euphotic zone and occurs from temperate to tropical waters (Bemis et al., 2000; Hemleben et al., 1989), while in the Mediterranean Sea it proliferates by the end of summer (Pujol and Grazzini, 1995). *Globorotalia inflata* and *G. truncatulinoides* are subsurface-dwelling species, which favor mixed conditions and cool water temperatures (Hemleben et al., 1989; Pujol and Grazzini, 1995). In the Mediterranean, both species are indicators of eutrophic conditions with a deeply mixed winter ocean layer (Rigual-Hernández et al., 2012; Rohling et al., 2004). *Globorotalia inflata* shows an opportunistic behavior in mesotrophic conditions (Chapman, 2010; Lončarić et al., 2007; Retailleau et al., 2011; Storz et al., 2009), and can be outnumbered by more opportunistic species such as *G. bulloides* in eutrophic environments. *Globigerina bulloides* thrives in high-productivity regions and is an indicator of upwelling intensity, responding to phytoplankton blooms and may outnumber species, which are adapted to less productive conditions (Conan et al., 2002; Schiebel et al., 2004; Thiede, 1975).

Higher percentages of warm water species *G. ruber*$_{SL}$ in the Alboran Sea might be explained by a narrower annual SST amplitude compared to the Balearic Sea (Fig. 1e), which favors the warm water species since SST is not falling below its specific temperature minimum limit of 14 °C (Bijma et al., 1990). Higher relative abundances of *G. truncatulinoides* in the Balearic Sea is of the same magnitude of those reported in the nearby Minorca Basin (Margaritelli et al., 2018). This abundance peak increases in coincidence of the Maunder Minimum event of the LIA, as in a wide portion of the central-western Mediterranean, and is due to the development of enhanced vertical mixing in winter (Margaritelli et al., 2020b). This interpretation is compatible with enhanced atmospheric circulation developed in close vicinity to the Gulf of Lion and its wind driven deep mixed conditions and/or a strong NC that may transport *G. truncatulinoides* to our study site (Fig. 1a). High relative abundances of *G. bulloides*, a species associated with periods of elevated primary productivity in the western Mediterranean Sea (Bárcena et al., 2004; Hernández-Almeida et al., 2011; Rigual-Hernández et al., 2012), demonstrate that the Balearic Sea is one of the most productive regions in the Mediterranean Sea (Stambler, 2014), although satellite data reveal that surface primary production may be even higher in the Alboran Basin (Fig. 1).

Great percentage values of non-target species in the Balearic Sea (Fig. 3g) are caused by high abundances of small sized species (150-250 μm; Dataset S1 & S2), dominated by *Neogloboquadrina incompta*. Its affinity to low-productive conditions with enhanced stratification of the surface water column (Schiebel and Hemleben, 2000) would explain the abundance pattern contrasting to the deep mixing indicator species *G. truncatulinoides*.

5.3.3. Planktic foraminiferal response to natural versus anthropogenic drivers

External forcing, like variations in solar activity and the cooling effect of sulphate aerosols expelled into the atmosphere after volcanic eruptions, are thought to be main mechanisms driving climate during the last millennium (Crowley, 2000; McGregor et al., 2015). These drivers influence large scale atmospheric patterns like NAO and AMO (IPCC, 2014), which in turn are associated with changes in climate and oceanographic conditions. Synchronously, anthropogenic induced climate change is responsible for almost half of the 20th century warming (Macías et al., 2013). Figs. 5 and 6 demonstrate how natural variability controls planktic foraminiferal species composition of the western Mediterranean Sea in pre-industrial times, whereas anthropogenic warming may lead to surface ocean productivity decline.

5.3.3.1. Natural variability as a driver in pre-industrial times (TSI, AMO). Decreasing solar activity revealed through increasing number and intensity of solar activity minima Maunder, Spörer and Wolf (Usoskin et al., 2016), and the more frequent occurrence of volcanic eruptions has led to a pronounced cooling since the MCA-LIA transition (Crowley and Unterman, 2013; McGregor et al., 2015). Decreasing SSTs in the western Mediterranean are closely linked to negative AMO phases during the LIA (Lüning et al., 2019), affecting water column properties mainly during summer seasons (Marullo et al., 2011; O'Reilly et al., 2017), triggering changes in planktic foraminiferal assemblages (Incarbona et al., 2019). During the second phase of the LIA, relative abundances of *G. ruber*$_{WHITE}$ decrease from ~8.1% to ~0.5% in the Balearic core (Fig. 3a). The surface-dwelling species, favoring warm, stratified waters was probably disadvantaged by decreasing SSTs and intensified vertical mixing of the water column. As winter SSTs are quite low at present, warm times with a monthly mean of 13.2 °C in February (Fig. 1e), winter months are expected to be colder during the LIA, with SSTs falling below temperature tolerance of *G. ruber*$_{WHITE}$ (Bijma et al., 1990), affecting standing stocks of this species even in summer. The drop in *G. ruber*$_{WHITE}$ is synchronous with an abundance increase of *G. inflata* and *G. truncatulinoides* (Fig. 3), two species associated with deep-winter mixing in this region (Rigual-Hernández et al., 2012). Results are supported by former studies in the Tyrrhenian Sea with a positive response of deep dwelling species during minimum solar activity during the LIA (Lirer et al., 2014; Margaritelli et al., 2018; Margaritelli et al., 2020b; Margaritelli et al., 2016). Increasing abundances of the deep dwelling species might indicate more intense vertical mixing during winter months, delaying the spring bloom and shortening the growing season for *G. ruber*$_{WHITE}$. It is not clear if reduced light levels during solar activity minima have a direct negative impact on the symbiont bearing species, since the species uses dinoflagellates for photosymbiosis (Hemleben et al., 1989).

During the older part of the Alboran record, percentage values of the warm water species G. ruber$_{WHITE}$ are in phase with $U^{k'}_{37}$ SST estimates likely driven by variabilities in AMO (Fig. 5). As a main representative of the summer assemblage (Bárcena et al., 2004), proliferation of G. ruber$_{WHITE}$ is favored by higher SST during the DA, whereas lower temperatures throughout the MCA result in a relative abundance drop. A prevailing negative AMO during the LIA is not recorded in G. ruber$_{WHITE}$. Instead, it increases its stock continuously in line with $U^{k'}_{37}$ SST in the Alboran Sea.

5.3.3.2. Natural variability as a driver for planktic foraminiferal population dynamics in pre-industrial times (NAO). Changes of climatologic and oceanographical conditions in the Mediterranean are closely linked to the boreal winter NAO index (Hurrell, 1995; Lionello et al., 2006; Nieto-Moreno et al., 2015; Schirrmacher et al., 2019; Tsimplis et al., 2013; Ulbrich et al., 2012), affecting phytoplankton and zooplankton communities through changes in ocean circulation and air-sea heat fluxes (Drinkwater et al., 2003), including plankton calcifier (Ausín et al., 2015; Bazzicalupo et al., 2020; Mojtahid et al., 2015). Long-term variability is displayed by planktic foraminiferal records, i.e. by ratios between indicators of eutrophic (*G. bulloides*) and deep-mixing (*G. inflata* and *G. truncatulinoides*) conditions, and the NAO and AMO (Figs. 5 & 6).

In the northwestern Mediterranean, *G. inflata* and *G. truncatulinoides* are associated with stronger winter mixing conditions (Rigual-Hernández et al., 2012). A relation between large scale atmospheric patterns and these species has been reported from the central Mediterranean Sea and is interpreted as changes in deep winter mixing (Incarbona et al., 2019). The flow of cold and dry air masses from continental regions into the western Mediterranean, which enhances heat loss and strengthens the NC circulation (Vignudelli et al., 1999), resulting in strong vertical mixing of water masses during WMDW formation in the Gulf of Lion

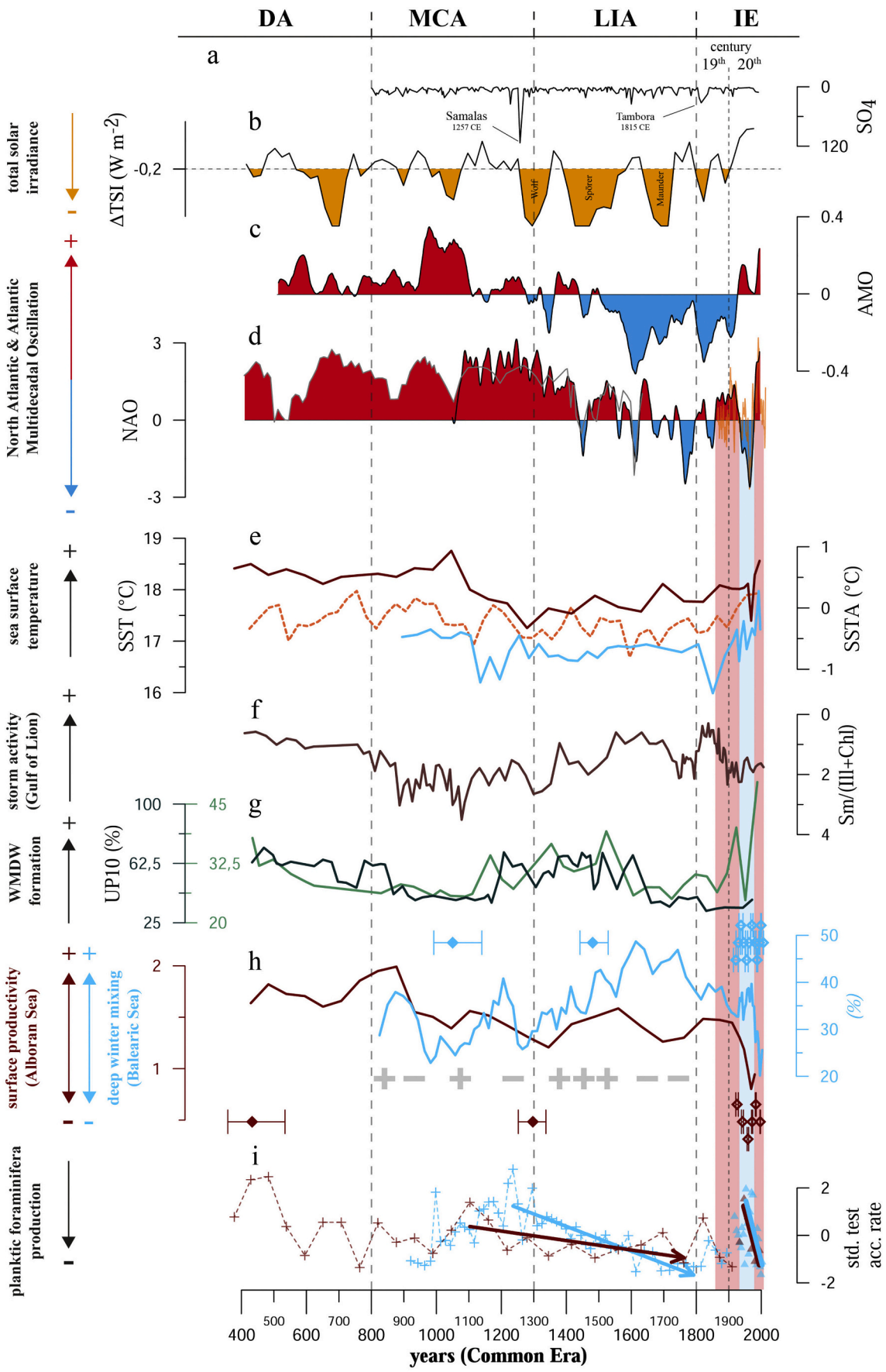

(caption on next page)

Fig. 5. Natural and anthropogenic forcing driving surface productivity and deep winter mixing in the western Mediterranean Sea during the Common Era expressed through planktic foraminiferal species composition and abundance changes. (a) Sulphate records in Antarctic and Greenland ice cores as a proxy for volcanic activity (Crowley and Unterman, 2013). (b) Total solar irradiance (TSI) based on ^{10}Be and ^{14}C data (Steinhilber et al., 2012; Steinhilber et al., 2009). Orange fillings indicate TSI periods below the mean (−0.2 W m^{-2}). (c) Reconstruction of Atlantic Multidecadal Oscillation (AMO) (Mann et al., 2009), expressed as 29 point moving average (dark line). (d) Reconstruction of North Atlantic Oscillation (NAO) through tree-ring and speleothem-based records (Trouet et al., 2009) expressed as 29 point moving average (dark line), lake sediment records as a grey line (Olsen et al., 2012) and instrumental data covering 1821 CE to 2013 CE (Jones et al., 1997) expressed as 5 point moving average (orange line). Positive and negative phases for NAO and AMO indices are highlighted as red and blue areas, above and below the mean. (e) Paleotemperature reconstruction for continental Europe as orange dashed line (Ahmed et al., 2013) and alkenone derived SST for Alboran (red) and Balearic (blue) cores. (f) Paleo storm activity in the Gulf of Lion (Sabatier et al., 2012). (g) Intensity of Western Mediterranean Deep-Water formation (WMDW), recorded through de-carbonated (green) and total (dark green) grain-size fraction (Cisneros et al., 2019). (h) Added relative abundance of *G. inflata* + *G. truncatulinoides* in the Balearic Sea (blue) as a proxy for deep winter mixing and *G. bulloides* versus *G. inflata* in the Alboran Sea (dark red) as a proxy for surface productivity. Grey plus and minus symbols indicate concurrent species composition changes at both study sites, related to (de-) and increasing phases of NAO modes on multidecadal time scales (i) Standardized total planktic foraminiferal test accumulation rate at the Alboran (red) and Balearic (blue) core sites: Crosses and dashed lines show values based on sedimentation rates rest upon ^{14}C dating. Triangles represent std. acc. rates based on sedimentation rates rest upon ^{210}Pb dating. Solid lines represent linear fit through LIA and 20th century second half, respectively. Filled and open diamonds represent ^{14}C dates and ^{210}Pb dates used as tie-points for age-depth model reconstruction, respectively, color coded by the corresponding core color (Alboran = red; Balearic = blue), including their associated 2σ errors. Duration of the Dark Age (DA), Medieval Climate Anomaly (MCA), Little Ice Age (LIA) and Industrial Era (IE) is based on estimates by Nieto-Moreno et al. (2011).

during winter months (Medoc, 1970; Mertens and Schott, 1998; Rohling et al., 2009). Cold and dry northerlies and north-westerlies, better known under the names Tramontana and Mistral, in particular during a negative phase of the East Atlantic Pattern, have the potential to cause intense heat loss, affecting dense water formation (DWF) in the Gulf of Lion (Josey et al., 2011). *Globorotalia truncatulinoides* inhabit subsurface waters most of their life span and migrate to surface waters for reproduction (Hemleben et al., 1989; Schiebel and Hemleben, 2005; Schiebel et al., 2002). Deep turbulent vertical mixing combined with a thermocline breakdown during the LIA, a period characterized by more negative NAO modes, may have caused proliferation of *G. truncatulinoides* and *G. inflata* in a shallower habitat. In contrast, stronger water column stratification as a result of lower surface heat loss during positive NAO and AMO phases during the MCA (Moreno et al., 2012) would have typically caused a subsurface habitat of *G. inflata* and *G. truncatulinoides*. During the first half of the LIA, relative abundances of *G. ruber*$_{\mathrm{WHITE}}$ are changing along with deep dwelling species, which is contradictory since the surface-dwelling species is a key indicator for water column stratification. As part of the summer assemblage, *G. ruber*$_{\mathrm{WHITE}}$ might have benefited by reduced surface production during LIA summer months, as reflected in test concentration and accumulation rates (Figs. 2 & 5). Intense vertical mixing during negative NAO phases might have delayed initiation of the spring bloom, shortening the growing season and decreasing phytoplankton abundance as hypothesized for regions in the North Atlantic (Dickson et al., 1988; Fromentin and Planque, 1996). In the northwestern Mediterranean Sea, katabatic wind bursts (Tramontana, Mistral) are associated with enhanced vertical mixing and reduced surface productivity (Keerthi et al., 2021). Due to its positive response to phytoplankton blooms in the northwestern Mediterranean (Rigual-Hernández et al., 2012), total planktic foraminiferal abundances, would decrease during years of intense winter mixing, resulting in enhanced relative stocks of *G. truncatulinoides* and *G. inflata*. Increasing total planktic foraminiferal stocks and low relative abundances of *G. truncatulinoides* and *G. inflata* would indicate a weakened DWF in the northwestern Mediterranean Sea. This is further supported by proxies describing the variability of paleo storm activity and deep water formation in the Northwestern Mediterranean throughout the Common Era (Cisneros et al., 2019; Sabatier et al., 2012). Prevailing negative NAO phases are associated with more intense storm activity, bringing cold katabatic winds over the Gulf of Lion and forcing intense vertical mixing and stimulating deep water formation in the northwestern Mediterranean Sea, explaining the enhanced abundances of *G. truncatulinoides* and *G. inflata* as a result of high vertical mixing.

At our study site in the western Alboran Sea, planktic foraminiferal assemblage composition is influenced by complex small-scale hydrographic conditions associated with NAO modes. On top of the multicentennial variation between MCA and LIA as described in the previous paragraph, selected species show a multidecadal variability (Fig. 5; plus and minus signs) in both records associated with changes in NAO modes. The in-phase pattern between the ratio of *G. bulloides* versus *G. inflata* in the Alboran record and the relative abundance changes of *G. truncatulinoides* and *G. inflata* in the Balearic core, is one of the most striking features of the record. As illustrated in Fig. 6, productivity changes in the Alboran Sea are strongly linked to DWF in the Gulf of Lion, both related to NAO variability (Fig. 5). Stronger WMDW formation results in deficit in surface water masses in the western Mediterranean Sea, which is compensated by stronger Atlantic surface water inflow through the SoG (Macías et al., 2016). This leads to higher velocities of the AJ, flowing in a northward direction along the Iberian Peninsula coast. Together with prevailing westerlies, this atmospheric and hydrographic concurrence is associated with highly fertile, nutrient rich coastal upwelling. A poor DWF with less pronounced westerlies would weaken the AJ, streaming further southward along the northern African coast, resulting in further offshore upwelling characterized by less fertile surface water conditions (Macías et al., 2008; Macías et al., 2007; Sarhan et al., 2000). Seasonal sediment trap data in the Alboran Sea (Bárcena et al., 2004) support the relation between Atlantic water inflow and planktic foraminiferal surface production. Specifically, G. *bulloides* is associated to high surface production and *G. inflata* is an indicator for less productive conditions. We suppose that a continuous strong AJ during times towards more positive NAO phases favors the occurrence of *G. bulloides* in the Alboran Sea as a result of high surface primary productivity, whereas a weak AJ during periods of decreasing NAO modes makes the Alboran Sea more meso- to oligotrophic, thus favoring *G. inflata* over *G. bulloides*.

The strong link between DWF in the Gulf of Lion and surface productivity in the Alboran Sea (Fig. 6) and its see-saw pattern related to NAO variability was previously described in Holocene marine records (Ausín et al., 2015; Bazzicalupo et al., 2020). There is still uncertainty as to which NAO mode is associated with reinforced WMDW formation and related surface productivity in the Alboran Sea. When looking at the multicenntenial variability described by *G. truncatulinoides* and *G. inflata* of the Balearic record, our data corroborate the assumption of Ausín et al. (2015) relating a negative NAO to enhanced northwesterlies and a strong WMDW formation, which is further supported by paleoenvironmental records covering the Late Holocene (Cacho et al., 2000; Schirrmacher et al., 2019). In contrast, Bazzicalupo et al. (2020) suggest that throughout the Holocene positive NAO phases were associated with strong northwesterlies which strengthen DWF and increase surface productivity in the Alboran basin, which is in accordance with the abundance changes on multidecadal time scales, which are in phase at both study sites (Fig. 5h). Recent hydrographic studies close to our core location support the hypothesis of Bazzicalupo et al. (2020) since upwelling intensity increased due to stronger westerly winds and an enhanced Atlantic Water inflow (Fenoglio-Marc et al., 2013; Vargas-Yáñez et al., 2008), thus enhancing productivity during the Dark Age

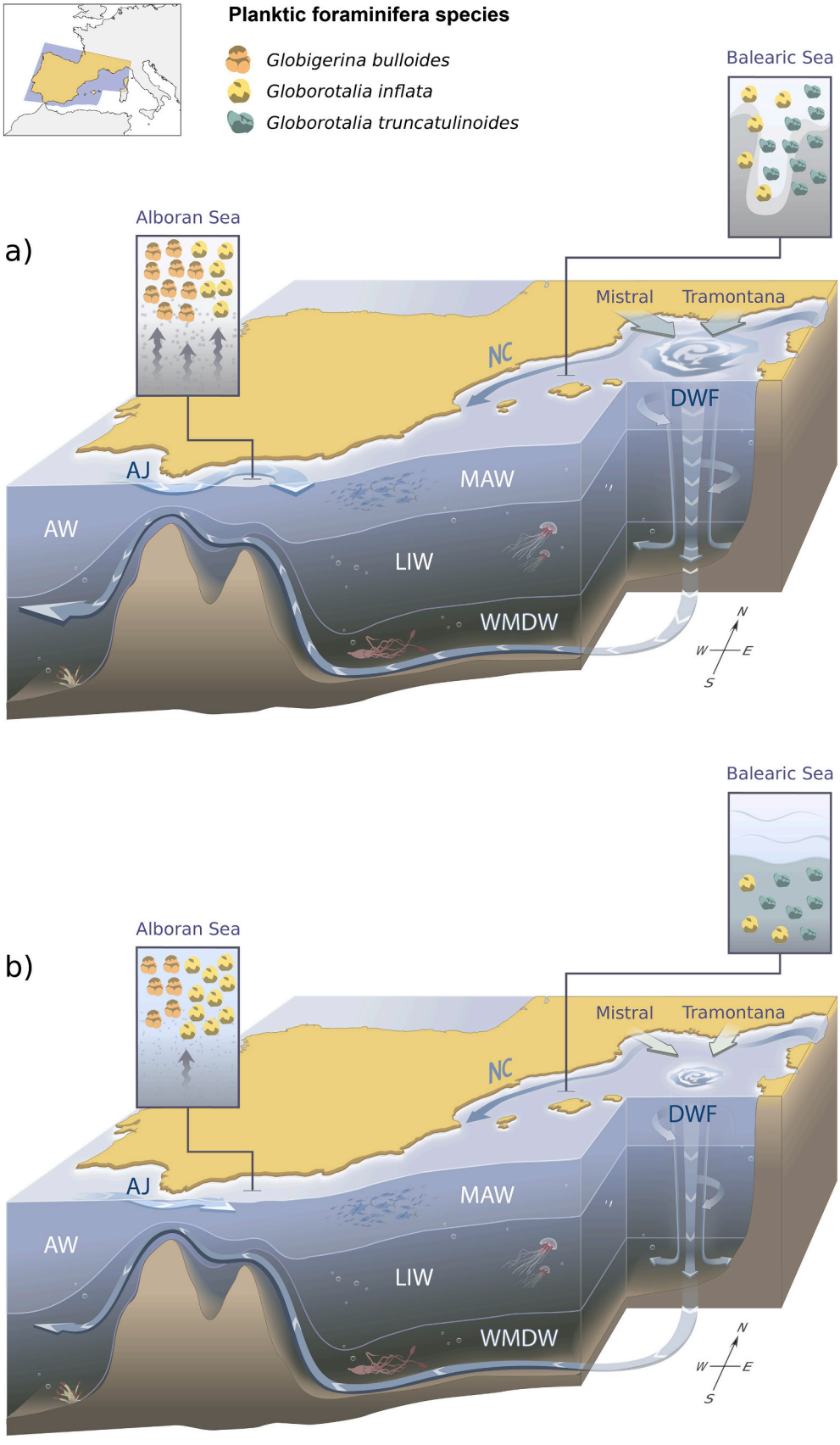

Fig. 6. Western Mediterranean circulation pattern and interaction with planktic foraminiferal community as explained in the text. (a) Enhanced northwesterly winds, deep water formation, strong Atlantic inflow inducing upwelling and increasing relative abundance of *G. bulloides* over *G. inflata* in the Alboran Sea, and *G. inflata* and *G. truncatulinoides* in the Balearic Sea. (b) Weakened northwesterly winds and deep water formation, lowering Atlantic inflow and reducing upwelling, increasing relative abundance of *G. inflata* over *G. bulloides* in the Alboran Sea, and decreasing percentages of *G. inflata* and *G. truncatulinoides* in the Balearic Sea (Figure by Jagoba Malumbres-Olarte).

and MCA (Nieto-Moreno et al., 2013). However, according to our data, the hypothesis of Bazzicalupo et al. (2020) may be applied to explain the multidecadal NAO variabilities during the Common Era, whereas findings of Ausín et al. (2015) are in good agreement with (paleo-) climatic and (paleo-) oceanographic processes stated above.

Additionally, the following reason may complicate a straightforward relation between western Mediterranean deep-water formation, Alboran Sea productivity and NAO variability. The main driver of WMDW formation could have changed from air-sea heat exchange during the MCA and LIA to buoyancy loss due to more arid climates during IE (Cisneros et al., 2019), explaining higher water fluxes through the Strait of Gibraltar during positive NAO indices (Fenoglio-Marc et al., 2013). Our findings do not contradict Mid-Pleistocene records, relating NAO+ phases to enhanced Alboran upwelling intensity and primary production (González-Lanchas et al., 2020), since they describe NAO phases with millennial cyclicity, whereas our cores cover higher temporal resolution. Additionally, complex interannual hydrographic variability (Peliz et al., 2013) relocating the high productive upwelling zones on a small spatial scale (Macías et al., 2008; Sarhan et al., 2000) and causing great interannual variability in the seasonal cycle of algal biomass (Bosc et al., 2004; D'Ortenzio and Ribera d'Alcalà, 2009) makes the Alboran Sea a challenging research site to study surface productivity changes (Bárcena et al., 2004; Mallo et al., 2017).

5.3.3.3. Anthropogenic warming as main driver in post-industrial times. In the Balearic and Alboran seas, a decrease of planktic foraminiferal production, test accumulation rates, and a rapid changing species assemblage are indicating an unprecedented reduction of WMDW formation and surface primary productivity during the 20th century. This is the first evidence of significant changes in planktic foraminiferal assemblages other than a geographical displacement of assemblages in the oceans and took place before the oldest survey used by Jonkers et al. (2019). Particularly, the drop of *G. bulloides* relative to *G. inflata* in the Alboran Sea over a period of low NAO indices during the first half of the 20th century, reveals depleting surface primary productivity, corroborated by decreasing alkenone concentrations recorded in the Alboran core at this time (Fig. 2b). In the Balearic Sea, declining abundances of *G. truncatulinoides* and *G. bulloides* during the second half of the 20th century, indicating reduced vertical mixing and lower surface productivity (Figs. 3 & 5h). During the same time period, SST shows unprecedented warming (Ahmed et al., 2013), as recorded in $U^{k'}_{37}$ SST estimates of both cores (discussed in 5.2) and more positive AMO phases (Figs. 5). These findings suggest that the western Mediterranean Sea became more oligotrophic during the 20th century, as a result of anthropogenically induced SST warming and vertical stratification of the surface water column. Primary productivity depends on light, and nutrient supply affected by stratification of the water column mostly driven by temperature (Longhurst, 1995). Higher SSTs increase near surface stratification inhibiting vertical mixing. Consequently, less nutrients are transported to the upper ocean causing less fertilized surface conditions (Behrenfeld et al., 2006). Lower primary production levels favor the proliferation of *G. inflata* over the high productivity indicator species *G. bulloides* (Fig. 5h). As the decrease in primary production cascades through the food web, total planktic foraminiferal abundance declines at 1953 ± 5 in the Balearic and at 1947 ± 3 CE in the Alboran Sea, manifested in decreases of test accumulation rates 10X and 25X faster than during the LIA respectively (Fig. 5i). This is in agreement with decreasing foraminiferal fluxes in the western Mediterranean Sea, when comparing plankton tow studies carried out from the late 1980s (Mallo et al., 2017; Pujol and Grazzini, 1995), and decreasing surface chlorophyll-a concentrations at both study sites during the last two decades (Fig. 1e).

These results differ from biogeochemical models and historical data suggesting an overall increase of surface primary productivity during the last century (Boyce et al., 2014; Macías et al., 2014). Marine productivity models show a positive trend taking the whole productive layer reaching depths of 200 m into account (von Schuckmann et al., 2020), whereas surface chlorophyll-a concentrations derived from satellites (Fig. 1) just represent the primary productivity of the upper surface layer. Surface dwellers as *G. bulloides* (Rebotim et al., 2017) respond to productivity changes in the upper surface layer. This would explain the low planktic foraminiferal summer production, despite the fact that summer is the most productive season in the Mediterranean Sea when considering the entire productive layer (von Schuckmann et al., 2020).

Interestingly, *G. ruber*$_{\mathrm{WHITE}}$ does not capture any warming signal at the beginning of the IE, but describing an abundance drop at both study sites. Negative excursions of *G. ruber*$_{\mathrm{WHITE}}$ during the same time period are detected at other regions in the western Mediterranean (Lirer et al., 2014; Margaritelli et al., 2016), suggesting a possible human overprint, manifested in changes of nutrient cycling in coastal areas. The onset of the Modern Warm Period starting around 1950 CE is characterized by a recovery of the warm water species, visible in both records.

Coccolithophore assemblages in the Alboran Sea core also testify a drastic environmental change since the IE. In the modern ocean, *Emiliania huxleyi* is the most common coccolithophore species, an opportunistic and r-selected taxon that rapidly responds to upper ocean nutrient supply (Young, 1994), and in the Alboran Sea the recent decrease in abundance suggests an overall decrease in productivity (Fig 2e). In the western Mediterranean, *Gephyrocpasa oceanica* is identified as a tracer of Atlantic surface water inflow through the Gibraltar Strait (Incarbona et al., 2008a; Knappertsbusch, 1993; Oviedo et al., 2015) and has indicated that the inflow of a sustained surface Atlantic water mass has increased in recent time, as a consequence of enhanced DWF (Nieto-Moreno et al. (2015), contradicting planktic foraminiferal composition changes in the western Mediterranean (Fig. 5h). In the temperate Northeastern Atlantic, *G. oceanica* has a clear affinity for oligotrophic warm waters (Bollmann, 1997; Ziveri et al., 2004) as suggested by the recent increase in abundance in our record (Fig. 2f). The opposite abundance changes of *E. huxleyi* and *G. oceanica* described in our record, can be interpreted as a response to decreased nutrient availability in the western Alboran Sea (Bárcena et al., 2004). *Florisphaera profunda* abundance is used generally to infer nutricline dynamics and productivity (Beaufort et al., 1997; Grelaud et al., 2012; Incarbona et al., 2008b; Molfino and McIntyre, 1990). However, a recent review points out that in the Mediterranean Sea, except for the Sicily Channel, the relationship with productivity levels is not clearly established (Hernández-Almeida et al., 2019). In particular, previous studies had shown that *F. profunda* can have different dynamics of deep production (Stoll et al., 2007) and this seems the case for the slight decrease of this taxa recorded in our core in recent years (Fig. 2g). In summary, we interpret *G. oceanica* abundance increases and *E. huxleyi* decreases in the top layer of the Alboran Sea sediment core as a reduction in surface productivity, which agrees with changes in planktic foraminiferal composition (Fig. 5). Remarkably, this study provides the first evidence of a distinct ecological modification in Mediterranean coccolithophore assemblages since industrial anthropogenic greenhouse gas emission.

6. Conclusions

We found that during pre-industrial times, planktic foraminiferal assemblages were strongly related to variabilities in NAO and AMO influenced by changes in solar irradiation. Positive NAO modes prevailed during the MCA and led to a weakened DWF in the Gulf of Lion. A predominant negative NAO during the LIA is associated with intense, cool northwesterly winds, reinforcing WMDW formation. A multidecadal variability is overlaying multicentennial variation, reflected in the species composition of both records showing lower surface productivity in the Alboran because of reduced DWF in the Gulf of Lion during times of declining NAO modes, and vice versa. The discrepancy between multidecadal and multicentennial responses of planktic foraminifera during the Common Era may not explain which NAO mode is

associated with reinforced DWF in the Gulf of Lion and related surface productivity in the western Alboran Sea. The pre-industrial signal of natural variability controlling the species composition and indicating sea surface productivity, is superimposed by anthropogenic warming during the 20th century. Increasing SSTs and enhanced vertical stratification since the second half of the last century has reduced marine surface productivity and resulted in a decrease of planktic foraminiferal production in the western Mediterranean Sea. Our results are supported by alkenone derived SST records at both sites showing an unprecedented increase of SST in the Anthropocene since about 1850 CE, which is remarkably in good accordance with instrumental data presenting 20th century warming and regional/global SST reconstructions. In pre-industrial times, both cores display warmer and colder sea surface conditions respectively during the MCA and the LIA, which is consistent with previous studies covering the Common Era.

Planktic foraminiferal assemblage composition is characteristic of climatic and oceanographic conditions prevailing at both study sites. Differences in total abundances mirror the distinct trophic conditions in the Balearic and Alboran seas. Relative abundances of *G. inflata* plus *G. truncatulinoides* might be used as a proxy for deep water formation intensity in the northwestern Mediterranean. Changing relative abundance between *G. bulloides* and *G. inflata* may be indicative of changes in the hydrographic conditions of the Alboran Gyre system driving surface ocean primary productivity.

Further investigations are needed to assess the effects of sea warming and changes in productivity on key marine planktic organisms and test production for the last centuries at different locations in the Mediterranean Sea, in particular since the semi-enclosed basin is known to be highly vulnerable and sensitive to alterations of the global climate. Further work is also required to better understand the mechanisms of deep-water formation in the entire Mediterranean Sea, including the eastern basin and the effects of large atmospheric patterns like NAO and AMO, to better predict changes in MTHC under anthropogenic climate change.

Declaration of Competing Interest

The authors declare that they have no known competing financial interests or personal relationships that could have appeared to influence the work reported in this paper.

Acknowledgments

We are grateful to George Kontakiotis and an anonymous reviewer for their helpful comments and suggestions. We thank the captain and crew of the Spanish R/V Ángeles Alvariño, and the researchers as part of the MedSeA cruise for supporting the sampling of this study. We thank Adam Subhas for conducting radiocarbon analysis at the NOSAMS facility at Woods Hole Oceanographic Institution (Massachusetts, USA). We also thank Marta Casado, Yolanda Gonzalez-Quinteiro, Bibiano Hortelano and Inma Fernandez for laboratory assistance, and Joan Manuel Bruach for his work on the analysis of ^{210}Pb. This work contributes to the ICTA-UAB "Unit of Excellence" (FPI/MDM-2015-0552-16-2; CEX2019-000940-M) and received further funding by the EU-FP7 "Mediterranean Sea Acidification in a Changing Climate" project (MedSeA; grant agreement 265103), the CALMED project (CTM2016-79547-R), and the Generalitat de Catalunya (MERS, 2014 SGR – 1356). The Spanish Ministry of Science and Innovation, Severo Ochoa Project CEX2018-000794-S is likewise acknowledged. The data used in this paper can be found in the supporting information and is uploaded online at the PANGAEA repository.

Appendix A. Supplementary data

Supplementary data to this article can be found online at https://doi.org/10.1016/j.gloplacha.2021.103549.

References

Abram, N.J., McGregor, H.V., Tierney, J.E., Evans, M.N., McKay, N.P., Kaufman, D.S., Gunten, L.v., 2016. Early onset of industrial-era warming across the oceans and continents. Nature 536, 411. https://doi.org/10.1038/nature19082.

Ahmed, M., Anchukaitis, K.J., Asrat, A., Borgaonkar, H.P., Braida, M., Buckley, B.M., Consortium, P.K., 2013. Continental-scale temperature variability during the past two millennia. Nat. Geosci. 6 (5), 339–346. https://doi.org/10.1038/ngeo1797.

Alves, E.Q., Macario, K., Ascough, P., Bronk Ramsey, C., 2018. The worldwide marine radiocarbon reservoir effect: definitions, mechanisms, and prospects. Rev. Geophys. 56 (1), 278–305. https://doi.org/10.1002/2017RG000588.

Anderson, O.R., Spindler, M., Bé, A.W.H., Hemleben, C., 1979. Trophic activity of planktonic foraminifera. J. Mar. Biol. Assoc. U. K. 59 (3), 791–799. https://doi.org/10.1017/S002531540004577X.

Appleby, P.G., Oldfield, F., 1992. Applications of lead-210 to sedimentation studies. In: Ivanovich, M., Harmon, R.S. (Eds.), Uranium series disequilibrium: applications to environmental problems, 2 ed. Clarendon Press, United Kingdom.

Ascough, P., Cook, G., Dugmore, A., 2005. Methodological approaches to determining the marine radiocarbon reservoir effect. Prog. Phys. Geogr. 29 (4), 532–547. https://doi.org/10.1191/0309133305pp461ra.

Ausín, B., Flores, J.A., Sierro, F.J., Cacho, I., Hernández-Almeida, I., Martrat, B., Grimalt, J.O., 2015. Atmospheric patterns driving Holocene productivity in the Alboran Sea (Western Mediterranean): a multiproxy approach. Holocene 25 (4), 583–595. https://doi.org/10.1177/0959683614565952.

Bárcena, M.A., Abrantes, F., 1998. Evidence of a high-productivity area off the coast of Málaga from studies of diatoms in surface sediments. Mar. Micropaleontol. 35 (1), 91–103. https://doi.org/10.1016/S0377-8398(98)00012-7.

Bárcena, M.A., Flores, J.A., Sierro, F.J., Pérez-Folgado, M., Fabres, J., Calafat, A., Canals, M., 2004. Planktonic response to main oceanographic changes in the Alboran Sea (Western Mediterranean) as documented in sediment traps and surface sediments. Mar. Micropaleontol. 53 (3–4), 423–445. https://doi.org/10.1016/j.marmicro.2004.09.009.

Barker, S., Broecker, W., Clark, E., Hajdas, I., 2007. Radiocarbon age offsets of foraminifera resulting from differential dissolution and fragmentation within the sedimentary bioturbated zone. Paleoceanogr. Paleoclimatol. 22 (2) https://doi.org/10.1029/2006PA001354.

Bauska, T.K., Joos, F., Mix, A.C., Roth, R., Ahn, J., Brook, E.J., 2015. Links between atmospheric carbon dioxide, the land carbon reservoir and climate over the past millennium. Nat. Geosci. 8 (5), 383–387. https://doi.org/10.1038/ngeo2422.

Bazzicalupo, P., Maiorano, P., Girone, A., Marino, M., Combourieu-Nebout, N., Pelosi, N., Incarbona, A., 2020. Holocene climate variability of the Western Mediterranean: surface water dynamics inferred from calcareous plankton assemblages. The Holocene 30 (5), 691–708. https://doi.org/10.1177/0959683619895580.

Bé, A.W.H., 1977. An ecological, zoogeographic and taxonomic review of recent planktonic foraminifera. Ocean. Micropaleontol. 1–100.

Bé, A.W.H., Tolderlund, D.S., 1971. Distribution and Ecology of Living Planktonic Foraminifera in Surface Waters of the Atlantic and Indian Ocean. In: Funnel, B.M., Riedel, W.R. (Eds.), The Micropaleontology of Oceans. University Press, New York, pp. 104–149.

Beaufort, L., Lancelot, Y., Camberlin, P., Cayre, O., Vincent, E., Bassinot, F., Labeyrie, L., 1997. Insolation cycles as a major control of equatorial Indian Ocean primary production. Science 278 (5342), 1451–1454. https://doi.org/10.1126/science.278.5342.1451.

Beaugrand, G., McQuatters-Gollop, A., Edwards, M., Goberville, E., 2013. Long-term responses of North Atlantic calcifying plankton to climate change. Nat. Clim. Chang. 3 (3), 263. https://doi.org/10.1038/nclimate1753.

Behrenfeld, M.J., O'Malley, R.T., Siegel, D.A., McClain, C.R., Sarmiento, J.L., Feldman, G.C., Boss, E.S., 2006. Climate-driven trends in contemporary ocean productivity. Nature 444 (7120), 752–755. https://doi.org/10.1038/nature05317.

Bemis, B.E., Spero, H.J., Lea, D.W., Bijma, J., 2000. Temperature influence on the carbon isotopic composition of Globigerina bulloides and Orbulina universa (planktonic foraminifera). Mar. Micropaleontol. 38 (3–4), 213–228. https://doi.org/10.1016/S0377-8398(00)00006-2.

Bianchi, C.N., 2007. Biodiversity issues for the forthcoming tropical Mediterranean Sea. Hydrobiologia 580 (1), 7. https://doi.org/10.1007/s10750-006-0469-5.

Bijma, J., Faber Jr., W.W., Hemleben, C., 1990. Temperature and salinity limits for growth and survival of some planktonic foraminifers in laboratory cultures. J. Foraminifer. Res. 20 (2), 95–116. https://doi.org/10.2113/gsjfr.20.2.95.

Blaauw, M., Christen, J.A., 2011. Flexible paleoclimate age-depth models using an autoregressive gamma process. Bayesian Anal. 6 (3), 457–474. https://doi.org/10.1214/11-BA618.

Bollmann, J., 1997. Morphology and biogeography of Gephyrocapsa coccoliths in Holocene sediments. Mar. Micropaleontol. 29 (3-4), 319–350. https://doi.org/10.1016/S0377-8398(96)00028-X.

Bormans, M., Garrett, C., 1989. A simple criterion for gyre formation by the surface outflow from a strait, with application to the Alboran Sea. J. Geophys. Res. Oceans 94 (C9), 12637–12644. https://doi.org/10.1029/JC094iC09p12637.

Bosc, E., Bricaud, A., Antoine, D., 2004. Seasonal and interannual variability in algal biomass and primary production in the Mediterranean Sea, as derived from 4 years of SeaWiFS observations. Glob. Biogeochem. Cycles 18 (1). https://doi.org/10.1029/2003GB002034.

Bown, P.R., Young, J.R., 1998. Techniques. In: Bown, P.R. (Ed.), Calcareous Nannofossil Biostratigraphy. Chapman and Hall, London, pp. 16–28.

Boyce, D.G., Dowd, M., Lewis, M.R., Worm, B., 2014. Estimating global chlorophyll changes over the past century. Prog. Oceanogr. 122, 163–173. https://doi.org/10.1016/j.pocean.2014.01.004.

Bradley, R.S., 2015. Chapter 3 - dating methods I. In: Bradley, R.S. (Ed.), Paleoclimatology, 3rd ed. Academic Press, San Diego, pp. 55–101.
Cacho, I., Grimalt, J.O., Pelejero, C., Canals, M., Sierro, F.J., Flores, J.A., Shackleton, N., 1999. Dansgaard-Oeschger and Heinrich event imprints in Alboran Sea paleotemperatures. Paleoceanogr. Paleoclimatol. 14 (6), 698–705. https://doi.org/10.1029/1999PA900044.
Cacho, I., Grimalt, J.O., Sierro, F.J., Shackleton, N., Canals, M., 2000. Evidence for enhanced Mediterranean thermohaline circulation during rapid climatic coolings. Earth Planet. Sci. Lett. 183 (3), 417–429. https://doi.org/10.1016/S0012-821X(00)00296-X.
Canals, M., Puig, P., de Madron, X.D., Heussner, S., Palanques, A., Fabres, J., 2006. Flushing submarine canyons. Nature 444 (7117), 354–357. https://doi.org/10.1038/nature05271.
Capotondi, L., Soroldoni, L., Principato, M.S., Corselli, C., 2004. Late Quaternary planktonic foraminiferal distributions: problems related to size fraction. In: Coccioni, R., Galeotti, S., Lirer, F. (Eds.), Proceedings of the First Italian Meeting on Environmental Micropaleontology. Grzybowski Foundation Special Publication, 9, pp. 1–6.
Chapman, M.R., 2010. Seasonal production patterns of planktonic foraminifera in the NE Atlantic Ocean: Implications for paleotemperature and hydrographic reconstructions. Paleoceanography 25 (1). https://doi.org/10.1029/2008PA001708.
Cisneros, M., Cacho, I., Frigola, J., Canals, M., Masqué, P., Martrat, B., Lirer, F., 2016. Sea surface temperature variability in the central-western Mediterranean Sea during the last 2700 years: a multi-proxy and multi-record approach. Clim. Past 12 (4), 849–869. https://doi.org/10.5194/cp-12-849-2016.
Cisneros, M., Cacho, I., Frigola, J., Sanchez-Vidal, A., Calafat, A., Pedrosa-Pàmies, R., Canals, M., 2019. Deep-water formation variability in the north-western Mediterranean Sea during the last 2500 yr: A proxy validation with present-day data. Glob. Planet. Chang. 177, 56–68. https://doi.org/10.1016/j.gloplacha.2019.03.012.
CLIMAP Project Members, Ruddiman, W.F., Cline, R.M.L., Hays, J.D., Prell, W.L., Ruddiman, W.F., Thompson, P.R., 1984. The last interglacial ocean. Quat. Res. 21 (2), 123–224. https://doi.org/10.1016/0033-5894(84)90098-X.
Colella, S., D'Ortenzio, F., Marullo, S., Santoleri, R., Ragni, M., d'Alcala, M.R., 2003. Primary Production Variability in the Mediterranean Sea from SeaWiFS Data. Paper presented at the Proceedings of SPIE.
Coma, R., Ribes, M., Serrano, E., Jiménez, E., Salat, J., Pascual, J., 2009. Global warming-enhanced stratification and mass mortality events in the Mediterranean. Proc. Natl. Acad. Sci. 106 (15), 6176–6181. https://doi.org/10.1073/pnas.0805801106.
Conan, S.M.H., Ivanova, E.M., Brummer, G.J.A., 2002. Quantifying carbonate dissolution and calibration of foraminiferal dissolution indices in the Somali Basin. Mar. Geol. 182 (3–4), 325–349. https://doi.org/10.1016/S0025-3227(01)00238-9.
Conte, M.H., Sicre, M.A., Rühlemann, C., Weber, J.C., Schulte, S., Schulz-Bull, D., Blanz, T., 2006. Global temperature calibration of the alkenone unsaturation index (UK′ 37) in surface waters and comparison with surface sediments. Geochem. Geophys. Geosyst. 7 (2) https://doi.org/10.1029/2005GC001054.
Cramer, W., Guiot, J., Fader, M., Garrabou, J., Gattuso, J.-P., Iglesias, A., Lange, M.A., Lionello, P., Llasat, M.C., Paz, S., Peñuelas, J., Snoussi, M., Toreti, Andrea, Tsimplis, M.N., Xoplaki, E., 2018. Climate change and interconnected risks to sustainable development in the Mediterranean. Nature Climate Chang. 8 (11), 972–980. https://doi.org/10.1038/s41558-018-0299-2.
Crowley, T.J., 2000. Causes of climate change over the past 1000 years. Science 289 (5477), 270–277. https://doi.org/10.1126/science.289.5477.270.
Crowley, T.J., Unterman, M.B., 2013. Technical details concerning development of a 1200 yr proxy index for global volcanism. Earth Syst. Sci. Data 5 (1), 187. https://doi.org/10.5194/essd-5-187-2013.
Crutzen, P.J., 2002. Geology of mankind. Nature 415 (6867), 23. https://doi.org/10.1038/415023a.
Di Donato, V., Daunis-i-Estadella, J., Martín-Fernández, J.A., Esposito, P., 2015. Size fraction effects on planktonic foraminifera assemblages: a compositional contribution to the Golden Sieve Rush. Math. Geosci. 47 (4), 455–470. https://doi.org/10.1007/s11004-014-9529-y.
Dickson, R.R., Kelly, P.M., Colebrook, J.M., Wooster, W.S., Cushing, D.H., 1988. North winds and production in the eastern North Atlantic. J. Plankton Res. 10 (1), 151–169. https://doi.org/10.1093/plankt/10.1.151.
D'Ortenzio, F., Ribera d'Alcalà, M., 2009. On the trophic regimes of the Mediterranean Sea: a satellite analysis. Biogeosciences 6 (2), 139–148. https://doi.org/10.5194/bg-6-139-2009.
Drinkwater, K.F., Belgrano, A., Borja, A., Conversi, A., Edwards, M., Greene, C.H., Walker, H., 2003. The response of marine ecosystems to climate variability associated with the North Atlantic Oscillation. In: Hurrell, J.W., Kushnir, Y., Ottersen, G., Visbeck, M. (Eds.), The North Atlantic Oscillation: Climatic Significance and Environmental Impact, pp. 211–234.
Eglinton, T.I., Conte, M.H., Eglinton, G., Hayes, J.M., 2001. Proceedings of a workshop on alkenone-based paleoceanographic indicators. Geochem. Geophys. Geosyst. 2 (1) https://doi.org/10.1029/2000gc000122.
Enfield, D.B., Mestas-Nuñez, A.M., Trimble, P.J., 2001. The Atlantic multidecadal oscillation and its relation to rainfall and river flows in the continental US. Geophys. Res. Lett. 28 (10), 2077–2080. https://doi.org/10.1029/2000GL012745.
Faust, J.C., Fabian, K., Milzer, G., Giraudeau, J., Knies, J., 2016. Norwegian fjord sediments reveal NAO related winter temperature and precipitation changes of the past 2800 years. Earth Planet. Sci. Lett. 435, 84–93. https://doi.org/10.1016/j.epsl.2015.12.003.
Fenoglio-Marc, L., Mariotti, A., Sannino, G., Meyssignac, B., Carillo, A., Struglia, M.V., Rixen, M., 2013. Decadal variability of net water flux at the Mediterranean Sea Gibraltar Strait. Glob. Planet. Chang. 100, 1–10. https://doi.org/10.1016/j.gloplacha.2012.08.007.
Field, D.B., Baumgartner, T.R., Charles, C.D., Ferreira-Bartrina, V., Ohman, M.D., 2006. Planktonic foraminifera of the California Current reflect 20th-century warming. Science 311 (5757), 63–66. https://doi.org/10.1126/science.1116220.
Flexas, M.M., Gomis, D., Ruiz, S., Pascual, A., León, P., 2006. In situ and satellite observations of the eastward migration of the Western Alboran Sea Gyre. Prog. Oceanogr. 70 (2), 486–509. https://doi.org/10.1016/j.pocean.2006.03.017.
Friedli, H., Lötscher, H., Oeschger, H., Siegenthaler, U., Stauffer, B., 1986. Ice core record of the 13C/12C ratio of atmospheric CO2 in the past two centuries. Nature 324 (6094), 237–238. https://doi.org/10.1038/324237a0.
Frigola, J., Moreno, A., Cacho, I., Canals, M., Sierro, F.J., Flores, J.A., Curtis, J.H., 2007. Holocene climate variability in the western Mediterranean region from a deepwater sediment record. Paleoceanography 22 (2). https://doi.org/10.1029/2006PA001307.
Fromentin, J.M., Planque, B., 1996. Calanus and environment in the eastern North Atlantic. II. Influence of the North Atlantic Oscillation on C. finmarchicus and C. helgolandicus. Mar. Ecol. Prog. Ser. 134, 111–118. https://doi.org/10.3354/meps134111.
Garcia-Gorriz, E., Carr, M.E., 2001. Physical control of phytoplankton distributions in the Alboran Sea: a numerical and satellite approach. J. Geophys. Res. Oceans 106 (C8), 16795–16805. https://doi.org/10.1029/1999JC000029.
Gascard, J.C., Richez, C., 1985. Water masses and circulation in the Western Alboran sea and in the Straits of Gibraltar. Prog. Oceanogr. 15 (3), 157–216. https://doi.org/10.1016/0079-6611(85)90031-X.
Giamali, C., Kontakiotis, G., Koskeridou, E., Ioakim, C., Antonarakou, A., 2020. Key environmental factors controlling planktonic foraminiferal and pteropod community's response to late quaternary hydroclimate changes in the South Aegean Sea (Eastern Mediterranean). J. Mar. Sci. Eng. 8 (9), 709.
Giorgi, F., 2006. Climate change hot-spots. Geophys. Res. Lett. 33 (8) https://doi.org/10.1029/2006gl025734.
Gleckler, P.J., Santer, B.D., Domingues, C.M., Pierce, D.W., Barnett, T.P., Church, J.A., Caldwell, P.M., 2012. Human-induced global ocean warming on multidecadal timescales. Nat. Clim. Chang. 2 (7), 524–529. https://doi.org/10.1038/nclimate1553.
Gogou, A., Triantaphyllou, M., Xoplaki, E., Izdebski, A., Parinos, C., Dimiza, M., Martrat, B., 2016. Climate variability and socio-environmental changes in the northern Aegean (NE Mediterranean) during the last 1500 years. Quat. Sci. Rev. 136, 209–228. https://doi.org/10.1016/j.quascirev.2016.01.009.
González-Lanchas, A., Flores, J.-A., Sierro, F.J., Bárcena, M.Á., Rigual-Hernández, A.S., Oliveira, D., Grimalt, J.O., 2020. A new perspective of the Alboran Upwelling System reconstruction during the Marine Isotope Stage 11: a high-resolution coccolithophore record. Quat. Sci. Rev. 245, 106520. https://doi.org/10.1016/j.quascirev.2020.106520.
Gray, S.T., Graumlich, L.J., Betancourt, J.L., Pederson, G.T., 2004. A tree-ring based reconstruction of the Atlantic Multidecadal Oscillation since 1567 AD. Geophys. Res. Lett. 31 (12) https://doi.org/10.1029/2004GL019932.
Grelaud, M., Marino, G., Ziveri, P., Rohling, E.J., 2012. Abrupt shoaling of the nutricline in response to massive freshwater flooding at the onset of the last interglacial sapropel event. Paleoceanography 27 (3). https://doi.org/10.1029/2012PA002288.
Heburn, G.W., La Violette, P.E., 1990. Variations in the structure of the anticyclonic gyres found in the Alboran Sea. J. Geophys. Res. Oceans 95 (C2), 1599–1613. https://doi.org/10.1029/JC095iC02p01599.
Hemleben, C., Spindler, M., Anderson, O.R., 1989. Modern Planktonic Foraminifera. Springer, New York, NY.
Hernández, A., Martin-Puertas, C., Moffa-Sánchez, P., Moreno-Chamarro, E., Ortega, P., Blockley, S., Xu, G., 2020. Modes of climate variability: synthesis and review of proxy-based reconstructions through the Holocene. Earth Sci. Rev. 103286. https://doi.org/10.1016/j.earscirev.2020.103286.
Hernández-Almeida, I., Bárcena, M.A., Flores, J.A., Sierro, F.J., Sanchez-Vidal, A., Calafat, A., 2011. Microplankton response to environmental conditions in the Alboran Sea (Western Mediterranean): one year sediment trap record. Mar. Micropaleontol. 78 (1–2), 14–24. https://doi.org/10.1016/j.marmicro.2010.09.005.
Hernández-Almeida, I., Ausín, B., Saavedra-Pellitero, M., Baumann, K.H., Stoll, H.M., 2019. Quantitative reconstruction of primary productivity in low latitudes during the last glacial maximum and the mid-to-late Holocene from a global Florisphaera profunda calibration dataset. Quat. Sci. Rev. 205, 166–181. https://doi.org/10.1016/j.quascirev.2018.12.016.
Hurrell, J.W., 1995. Decadal trends in the North Atlantic Oscillation: regional temperatures and precipitation. Science 269 (5224), 676–679. https://doi.org/10.1126/science.269.5224.676.
Hurrell, J.W., 2020. The Climate Data Guide: Hurrell North Atlantic Oscillation (NAO) Index (Station-Based). Last Modified 24 Apr 2020. Retrieved from. https://climatedataguide.ucar.edu/climate-data/hurrell-north-atlantic-oscillation-nao-index-station-based.
Incarbona, A., Bonomo, S., Di Stefano, E., Zgozi, S., Essarbout, N., Talha, M., Placenti, F., 2008a. Calcareous nannofossil surface sediment assemblages from the sicily channel (central Mediterranean Sea): palaeoceanographic implications. Mar. Micropaleontol. 67 (3-4), 297–309. https://doi.org/10.1016/j.marmicro.2008.03.001.
Incarbona, A., Di Stefano, E., Patti, B., Pelosi, N., Bonomo, S., Mazzola, S., Bonanno, A., 2008b. Holocene millennial-scale productivity variations in the sicily channel (Mediterranean Sea). Paleoceanography 23 (3). https://doi.org/10.1029/2007PA001581.
Incarbona, A., Jonkers, L., Ferraro, S., Sprovieri, R., Tranchida, G., 2019. Sea surface temperatures and paleoenvironmental variability in the central Mediterranean

during historical times reconstructed using planktonic foraminifera. Paleoceanogr. Paleoclimatol. 34 (3), 394–408. https://doi.org/10.1029/2018PA003529.
IPCC, 2014. Information from Paleoclimate Archives. In: Climate Change 2013 – The Physical Science Basis: Working Group I Contribution to the Fifth Assessment Report of the Intergovernmental Panel on Climate Change. Cambridge University Press, Cambridge, pp. 383–464.
Jentzen, A., Schönfeld, J., Schiebel, R., 2018. Assessment of the effect of increasing temperature on the ecology and assemblage structure of modern planktic foraminifers in the Caribbean and surrounding seas. J. Foraminifer. Res. 48 (3), 251–272. https://doi.org/10.2113/gsjfr.48.3.251.
Jones, P.D., Jonsson, T., Wheeler, D., 1997. Extension to the North Atlantic oscillation using early instrumental pressure observations from Gibraltar and south-west Iceland. Int. J. Climatol. 17 (13), 1433–1450. https://doi.org/10.1002/(SICI)1097-0088(19971115)17:13<1433::AID-JOC203>3.0.CO;2-P.
Jonkers, L., Hillebrand, H., Kucera, M., 2019. Global change drives modern plankton communities away from the pre-industrial state. Nature 570 (7761), 372–375. https://doi.org/10.1038/s41586-019-1230-3.
Josey, S.A., Somot, S., Tsimplis, M., 2011. Impacts of atmospheric modes of variability on Mediterranean Sea surface heat exchange. J. Geophys. Res. Oceans 116 (C2). https://doi.org/10.1029/2010jc006685.
Kaplan, A., Cane, M.A., Kushnir, Y., Clement, A.C., Blumenthal, M.B., Rajagopalan, B., 1998. Analyses of global sea surface temperature 1856–1991. J. Geophys. Res. Oceans 103 (C9), 18567–18589. https://doi.org/10.1029/97JC01736.
Keerthi, M.G., Lévy, M., Aumont, O., 2021. Intermittency in phytoplankton bloom triggered by modulations in vertical stability. Sci. Rep. 11 (1), 1285. https://doi.org/10.1038/s41598-020-80331-z.
Knappertsbusch, M., 1993. Geographic distribution of living and Holocene coccolithophores in the Mediterranean Sea. Mar. Micropaleontol. 21 (1-3), 219–247. https://doi.org/10.1016/0377-8398(93)90016-Q.
Kontakiotis, G., Karakitsios, V., Mortyn, P.G., Antonarakou, A., Drinia, H., Anastasakis, G., De Rafelis, M., 2016. New insights into the early Pliocene hydrographic dynamics and their relationship to the climatic evolution of the Mediterranean Sea. Palaeogeogr. Palaeoclimatol. Palaeoecol. 459, 348–364. https://doi.org/10.1016/j.palaeo.2016.07.025.
Kontakiotis, G., Antonarakou, A., Mortyn, P.G., Drinia, H., Anastasakis, G., Zarkogiannis, S., Möbius, J., 2017. Morphological recognition of Globigerinoides ruber morphotypes and their susceptibility to diagenetic alteration in the eastern Mediterranean Sea. J. Mar. Syst. 174, 12–24. https://doi.org/10.1016/j.jmarsys.2017.05.005.
Krishnaswamy, S., Lal, D., Martin, J.M., Meybeck, M., 1971. Geochronology of lake sediments. Earth Planet. Sci. Lett. 11 (1–5), 407–414. https://doi.org/10.1016/0012-821X(71)90202-0.
Kucera, M., 2007. Chapter six planktonic foraminifera as tracers of past oceanic environments. In: Hillaire-Marcel, C., De Vernal, A. (Eds.), Developments in Marine Geology, 1. Elsevier, pp. 213–262.
La Violette, P.E., 1990. The western Mediterranean circulation experiment (WMCE): introduction. J. Geophys. Res. Oceans 95 (C2), 1511–1514. https://doi.org/10.1029/JC095iC02p01511.
Lejeusne, C., Chevaldonné, P., Pergent-Martini, C., Boudouresque, C.F., Pérez, T., 2010. Climate change effects on a miniature ocean: the highly diverse, highly impacted Mediterranean Sea. Trends Ecol. Evol. 25 (4), 250–260. https://doi.org/10.1016/j.tree.2009.10.009.
Li, G., Cheng, L., Zhu, J., Trenberth, K.E., Mann, M.E., Abraham, J.P., 2020. Increasing ocean stratification over the past half-century. Nat. Clim. Chang. 10 (12), 1116–1123. https://doi.org/10.1038/s41558-020-00918-2.
Lionello, P., Malanotte-Rizzoli, P., Boscolo, R., Alpert, P., Artale, V., Li, L., Xoplaki, E., 2006. The Mediterranean climate: an overview of the main characteristics and issues. In: Lionello, P., Malanotte-Rizzoli, P., Boscolo, R. (Eds.), Developments in Earth and Environmental Sciences, 4. Elsevier, pp. 1–26.
Lirer, F., Sprovieri, M., Vallefuoco, M., Ferraro, L., Pelosi, N., Giordano, L., Capotondi, L., 2014. Planktonic foraminifera as bio-indicators for monitoring the climatic changes that have occurred over the past 2000 years in the southeastern Tyrrhenian Sea. Integr. Zool. 9 (4), 542–554. https://doi.org/10.1111/1749-4877.12083.
Lončarić, N., van Iperen, J., Kroon, D., Brummer, G.-J.A., 2007. Seasonal export and sediment preservation of diatomaceous, foraminiferal and organic matter mass fluxes in a trophic gradient across the SE Atlantic. Prog. Oceanogr. 73 (1), 27–59. https://doi.org/10.1016/j.pocean.2006.10.008.
Longhurst, A., 1995. Seasonal cycles of pelagic production and consumption. Prog. Oceanogr. 36 (2), 77–167. https://doi.org/10.1016/0079-6611(95)00015-1.
Lüning, S., Schulte, L., Garcés-Pastor, S., Danladi, I.B., Gałka, M., 2019. The Medieval climate anomaly in the Mediterranean region. Paleoceanogr. Paleoclimatol. 34 (10), 1625–1649. https://doi.org/10.1029/2019pa003734.
Macías, D.M., Navarro, G., Echevarría, F., García, C., Cueto, J., 2007. Phytoplankton pigment distribution in the northwestern Alboran Sea and meteorological forcing: a remote sensing study. J. Mar. Res. 65 (4), 523–543. https://doi.org/10.1357/002224007782689085.
Macías, D.M., Bruno, M., Echevarría, F., Vázquez, A., García, C.M., 2008. Meteorologically-induced mesoscale variability of the North-western Alboran Sea (southern Spain) and related biological patterns. Estuar. Coast. Shelf Sci. 78 (2), 250–266. https://doi.org/10.1016/j.ecss.2007.12.008.
Macías, D.M., Garcia-Gorriz, E., Stips, A., 2013. Understanding the causes of recent warming of Mediterranean waters. How much could be attributed to climate change? PLoS One 8 (11), e81591. https://doi.org/10.1371/journal.pone.0081591.
Macías, D.M., Garcia-Gorriz, E., Piroddi, C., Stips, A., 2014. Biogeochemical control of marine productivity in the Mediterranean Sea during the last 50 years. Glob. Biogeochem. Cycles 28 (8), 897–907. https://doi.org/10.1002/2014GB004846.
Macías, D.M., Garcia-Gorriz, E., Stips, A., 2015. Productivity changes in the Mediterranean Sea for the twenty-first century in response to changes in the regional atmospheric forcing. Front. Mar. Sci. 2 (79) https://doi.org/10.3389/fmars.2015.00079.
Macías, D.M., Garcia-Gorriz, E., Stips, A., 2016. The seasonal cycle of the Atlantic Jet dynamics in the Alboran Sea: direct atmospheric forcing versus Mediterranean thermohaline circulation. Ocean Dyn. 66 (2), 137–151. https://doi.org/10.1007/s10236-015-0914-y.
Mallo, M., Ziveri, P., Mortyn, P.G., Schiebel, R., Grelaud, M., 2017. Low planktic foraminiferal diversity and abundance observed in a spring 2013 west-east Mediterranean Sea plankton tow transect. Biogeosciences 14 (9). https://doi.org/10.5194/bg-14-2245-2017.
Mann, M.E., Zhang, Z., Rutherford, S., Bradley, R.S., Hughes, M.K., Shindell, D., Ni, F., 2009. Global signatures and dynamical origins of the little ice age and medieval climate anomaly. Science 326 (5957), 1256–1260. https://doi.org/10.1126/science.1177303.
Margaritelli, G., Vallefuoco, M., Di Rita, F., Capotondi, L., Bellucci, L.G., Insinga, D.D., Lirer, F., 2016. Marine response to climate changes during the last five millennia in the central Mediterranean Sea. Glob. Planet. Chang. 142, 53–72. https://doi.org/10.1016/j.gloplacha.2016.04.007.
Margaritelli, G., Cisneros, M., Cacho, I., Capotondi, L., Vallefuoco, M., Rettori, R., Lirer, F., 2018. Climatic variability over the last 3000 years in the central - western Mediterranean Sea (Menorca Basin) detected by planktonic foraminifera and stable isotope records. Glob. Planet. Chang. 169, 179–187. https://doi.org/10.1016/j.gloplacha.2018.07.012.
Margaritelli, G., Cacho, I., Català, A., Barra, M., Bellucci, L.G., Lubritto, C., Lirer, F., 2020a. Persistent warm Mediterranean surface waters during the Roman period. Sci. Rep. 10 (1), 10431. https://doi.org/10.1038/s41598-020-67281-2.
Margaritelli, G., Lirer, F., Schroeder, K., Alberico, I., Dentici, M.P., Caruso, A., 2020b. Globorotalia truncatulinoides in Central - Western Mediterranean Sea during the Little Ice Age. Mar. Micropaleontol. 161, 101921. https://doi.org/10.1016/j.marmicro.2020.101921.
Martrat, B., Grimalt, J.O., Lopez-Martinez, C., Cacho, I., Sierro, F.J., Flores, J.A., Hodell, D.A., 2004. Abrupt temperature changes in the Western Mediterranean over the past 250,000 years. Science 306 (5702), 1762–1765. https://doi.org/10.1126/science.1101706.
Martrat, B., Jimenez-Amat, P., Zahn, R., Grimalt, J.O., 2014. Similarities and dissimilarities between the last two deglaciations and interglaciations in the North Atlantic region. Quat. Sci. Rev. 99, 122–134. https://doi.org/10.1016/j.quascirev.2014.06.016.
Marullo, S., Artale, V., Santoleri, R., 2011. The SST multidecadal variability in the Atlantic–Mediterranean region and its relation to AMO. J. Clim. 24 (16), 4385–4401. https://doi.org/10.1175/2011JCLI3884.1.
Masqué, P., Fabres, J., Canals, M., Sanchez-Cabeza, J., Sanchez-Vidal, A., Cacho, I., Bruach, J., 2003. Accumulation rates of major constituents of hemipelagic sediments in the deep Alboran Sea: a centennial perspective of sedimentary dynamics. Mar. Geol. 193 (3-4), 207–233. https://doi.org/10.1016/S0025-3227(02)00593-5.
McGregor, H.V., Evans, M.N., Goosse, H., Leduc, G., Martrat, B., Addison, J.A., Ersek, V., 2015. Robust global ocean cooling trend for the pre-industrial Common Era. Nat. Geosci. 8 (9), 671–677. https://doi.org/10.1038/ngeo2510.
Medoc, G., 1970. Observation of formation of deep water in the Mediterranean Sea, 1969. Nature 227 (5262), 1037–1040. https://doi.org/10.1038/2271037a0.
Mekik, F., 2014. Radiocarbon dating of planktonic foraminifer shells: a cautionary tale. Paleoceanogr. Paleoclimatol. 29 (1), 13–29. https://doi.org/10.1002/2013PA002532.
Mertens, C., Schott, F., 1998. Interannual variability of deep-water formation in the northwestern Mediterranean. J. Phys. Oceanogr. 28 (7), 1410–1424. https://doi.org/10.1175/1520-0485(1998)028<1410:Ivodwf>2.0.Co;2.
Millero, F.J., Morse, J., Chen, C.-T., 1979. The carbonate system in the western Mediterranean Sea. Deep Sea Res. Part A Oceanogr. Res. Pap. 26 (12), 1395–1404. https://doi.org/10.1016/0198-0149(79)90007-4.
Millot, C., 1999. Circulation in the Western Mediterranean Sea. J. Mar. Syst. 20 (1), 423–442. https://doi.org/10.1016/S0924-7963(98)00078-5.
Mojtahid, M., Manceau, R., Schiebel, R., Hennekam, R., de Lange, G.J., 2015. Thirteen thousand years of southeastern Mediterranean climate variability inferred from an integrative planktic foraminiferal-based approach. Paleoceanography 30 (4), 402–422. https://doi.org/10.1002/2014pa002705.
Molfino, B., McIntyre, A., 1990. Precessional forcing of nutricline dynamics in the equatorial Atlantic. Science 249 (4970), 766–769. https://doi.org/10.1126/science.249.4970.766.
Moreno, A., Pérez, A., Frigola, J., Nieto-Moreno, V., Rodrigo-Gámiz, M., Martrat, B., Valero-Garcés, B.L., 2012. The Medieval Climate Anomaly in the Iberian Peninsula reconstructed from marine and lake records. Quat. Sci. Rev. 43, 16–32. https://doi.org/10.1016/j.quascirev.2012.04.007.
Morey, A.E., Mix, A.C., Pisias, N.G., 2005. Planktonic foraminiferal assemblages preserved in surface sediments correspond to multiple environment variables. Quat. Sci. Rev. 24 (7), 925–950. https://doi.org/10.1016/j.quascirev.2003.09.011.
Nieto-Moreno, V., Martínez-Ruiz, F., Giralt, S., Jiménez-Espejo, F., Gallego-Torres, D., Rodrigo-Gámiz, M., De Lange, G., 2011. Tracking climate variability in the western Mediterranean during the Late Holocene: a multiproxy approach. Clim. Past 7 (4), 1395–1414. https://doi.org/10.5194/cpd-7-635-2011.
Nieto-Moreno, V., Martínez-Ruiz, F., Willmott, V., García-Orellana, J., Masqué, P., Damsté, J.S., 2013. Climate conditions in the westernmost Mediterranean over the last two millennia: an integrated biomarker approach. Org. Geochem. 55, 1–10. https://doi.org/10.1016/j.orggeochem.2012.11.001.

NASA Goddard Space Flight Center, O. E. L., Ocean Biology Processing Group, 2020. Moderate-resolution Imaging Spectroradiometer (MODIS) Aqua Chlorophyll Data; 2018 Reprocessing. NASA OB.DAAC, Greenbelt, MD, USA.
Nieto-Moreno, V., Martínez-Ruiz, F., Gallego-Torres, D., Giralt, S., García-Orellana, J., Masque, P., Ortega-Huertas, M., 2015. Palaeoclimate and palaeoceanographic conditions in the westernmost Mediterranean over the last millennium: an integrated organic and inorganic approach. J. Geol. Soc. 172 (2), 264–271. https://doi.org/10.1144/jgs2013-105.
Nittrouer, C.A., DeMaster, D.J., McKee, B.A., Cutshall, N.H., Larsen, I.L., 1984. The effect of sediment mixing on Pb-210 accumulation rates for the Washington continental shelf. Mar. Geol. 54 (3), 201–221. https://doi.org/10.1016/0025-3227(84)90038-0.
Numberger, L., Hemleben, C., Hoffmann, R., Mackensen, A., Schulz, H., Wunderlich, J.-M., Kucera, M., 2009. Habitats, abundance patterns and isotopic signals of morphotypes of the planktonic foraminifer Globigerinoides ruber (d'Orbigny) in the eastern Mediterranean Sea since the Marine Isotopic Stage 12. Mar. Micropaleontol. 73 (1-2), 90–104. https://doi.org/10.1016/j.marmicro.2009.07.004.
O'Reilly, C.H., Woollings, T., Zanna, L., 2017. The dynamical influence of the Atlantic Multidecadal Oscillation on continental climate. J. Clim. 30 (18), 7213–7230. https://doi.org/10.1175/JCLI-D-16-0345.1.
Olsen, J., Anderson, N.J., Knudsen, M.F., 2012. Variability of the North Atlantic Oscillation over the past 5,200 years. Nat. Geosci. 5 (11), 808–812. https://doi.org/10.1038/ngeo1589.
Osborn, T.J., 2004. Simulating the winter North Atlantic Oscillation: the roles of internal variability and greenhouse gas forcing. Clim. Dyn. 22 (6–7), 605–623. https://doi.org/10.1007/s00382-004-0405-1.
Oviedo, A., Ziveri, P., Álvarez, M., Tanhua, T., 2015. Is coccolithophore distribution in the Mediterranean Sea related to seawater carbonate chemistry? Ocean Sci. 11 (1), 13–32. https://doi.org/10.5194/os-11-13-2015.
Peliz, A., Boutov, D., Teles-Machado, A., 2013. The Alboran Sea mesoscale in a long term high resolution simulation: statistical analysis. Ocean Model. 72, 32–52. https://doi.org/10.1016/j.ocemod.2013.07.002.
Pérez-Folgado, M., Sierro, F.J., Flores, J.A., Cacho, I., Grimalt, J.O., Zahn, R., Shackleton, N., 2003. Western Mediterranean planktonic foraminifera events and millennial climatic variability during the last 70 kyr. Mar. Micropaleontol. 48 (1), 49–70. https://doi.org/10.1016/S0377-8398(02)00160-3.
Philippart, C.J.M., Anadón, R., Danovaro, R., Dippner, J.W., Drinkwater, K.F., Hawkins, S.J., Reid, P.C., 2011. Impacts of climate change on European marine ecosystems: observations, expectations and indicators. J. Exp. Mar. Biol. Ecol. 400 (1), 52–69. https://doi.org/10.1016/j.jembe.2011.02.023.
Philippsen, B., 2013. The freshwater reservoir effect in radiocarbon dating. Heritage Sci. 1 (1), 24. https://doi.org/10.1186/2050-7445-1-24.
Puig, P., Masqué, P., Martín, J., Paradis, S., Juan-Dfaz, X., Toro, M., Palanques, A., 2015. Changes in sediment accumulation rates within NW Mediterranean submarine canyons caused by bottom trawling activities. In: Briand, F. (Ed.), Submarine Canyon Dynamics in the Mediterranean and Tributary Seas - An Integrated Geological, Oceanographic and Biological Perspective. CIESM Publisher, Monaco, p. 232. Vol. CIESM Monograph 47.
Pujol, C., Grazzini, C.V., 1995. Distribution patterns of live planktic foraminifers as related to regional hydrography and productive systems of the Mediterranean Sea. Mar. Micropaleontol. 25 (2), 187–217. https://doi.org/10.1016/0377-8398(95)00002-I.
Rayner, N., Parker, D.E., Horton, E., Folland, C.K., Alexander, L.V., Rowell, D., Kaplan, A., 2003. Global analyses of sea surface temperature, sea ice, and night marine air temperature since the late nineteenth century. J. Geophys. Res.-Atmos. 108 (D14) https://doi.org/10.1029/2002JD002670.
Rebotim, A., Voelker, A.H., Jonkers, L., Waniek, J.J., Meggers, H., Schiebel, R., Kucera, M., 2017. Factors controlling the depth habitat of planktonic foraminifera in the subtropical eastern North Atlantic. Biogeosciences 14 (4), 827–859. https://doi.org/10.5194/bg-14-827-2017.
Reimer, P.J., Bard, E., Bayliss, A., Beck, J.W., Blackwell, P.G., Ramsey, C.B., Friedrich, M., 2013. IntCal13 and Marine13 radiocarbon age calibration curves 0–50,000 years cal BP. Radiocarbon 55 (4), 1869–1887. https://doi.org/10.2458/azu_js_rc.55.16947.
Renault, L., Oguz, T., Pascual, A., Vizoso, G., Tintoré, J., 2012. Surface circulation in the Alborán Sea (western Mediterranean) inferred from remotely sensed data. J. Geophys. Res. Oceans 117 (C8). https://doi.org/10.1029/2011JC007659.
Retailleau, S., Schiebel, R., Howa, H., 2011. Population dynamics of living planktic foraminifers in the hemipelagic southeastern Bay of Biscay. Mar. Micropaleontol. 80 (3), 89–100. https://doi.org/10.1016/j.marmicro.2011.06.003.
Reynolds, R.W., Smith, T.M., 1994. Improved global sea surface temperature analyses using optimum interpolation. J. Clim. 7 (6), 929–948. https://doi.org/10.1175/1520-0442(1994)007<0929:IGSSTA>2.0.CO;2.
Rigual-Hernández, A.S., Sierro, F.J., Bárcena, M.A., Flores, J.A., Heussner, S., 2012. Seasonal and interannual changes of planktic foraminiferal fluxes in the Gulf of Lions (NW Mediterranean) and their implications for paleoceanographic studies: two 12-year sediment trap records. Deep-Sea Res. I Oceanogr. Res. Pap. 66, 26–40. https://doi.org/10.1016/j.dsr.2012.03.011.
Robbins, J.A., 1978. Geochemical and geophysical applications of radioactive lead. In: Nriagu, J.O. (Ed.), Biogeochemistry of Lead in the Environment. Elsevier Scientific, Amsterdam, pp. 285–393.
Rohling, E.J., Sprovieri, M., Cane, T., Casford, J.S.L., Cooke, S., Bouloubassi, I., Kroon, D., 2004. Reconstructing past planktic foraminiferal habitats using stable isotope data: a case history for Mediterranean sapropel S5. Mar. Micropaleontol. 50 (1), 89–123. https://doi.org/10.1016/S0377-8398(03)00068-9.
Rohling, E.J., Abu-Zied, R., Casford, J., Hayes, A., Hoogakker, B., 2009. The marine environment: present and past. In: Woodward, J.C. (Ed.), The Physical Geography of the Mediterranean, 8. Oxford University Press, Oxford, pp. 33–67.
Rutherford, S., D'Hondt, S., Prell, W., 1999. Environmental controls on the geographic distribution of zooplankton diversity. Nature 400 (6746), 749–753. https://doi.org/10.1038/23449.
Sabatier, P., Dezileau, L., Colin, C., Briqueu, L., Bouchette, F., Martinez, P., Von Grafenstein, U., 2012. 7000 years of paleostorm activity in the NW Mediterranean Sea in response to Holocene climate events. Quat. Res. 77 (1), 1–11. https://doi.org/10.1016/j.yqres.2011.09.002.
Sánchez-Cabeza, J., Masqué, P., Ani-Ragolta, I., 1998. 210Pb and210Po analysis in sediments and soils by microwave acid digestion. J. Radioanal. Nucl. Chem. 227 (1-2), 19–22. https://doi.org/10.1007/bf02386425.
Sarhan, T., Garcia, X., Lafuente, J., Vargas, M., Vargas, J.M., Plaza, F., 2000. Upwelling mechanisms in the northwestern Alboran Sea. J. Mar. Syst. 23 (4), 317–331. https://doi.org/10.1016/S0924-7963(99)00068-8.
Schiebel, R., Hemleben, C., 2000. Interannual variability of planktic foraminiferal populations and test flux in the eastern North Atlantic Ocean (JGOFS). Deep-Sea Res. II Top. Stud. Oceanogr. 47 (9), 1809–1852. https://doi.org/10.1016/S0967-0645(00)00008-4.
Schiebel, R., Hemleben, C., 2005. Modern planktic foraminifera. Paläontol. Z. 79 (1), 135–148. https://doi.org/10.1007/BF03021758.
Schiebel, R., Hemleben, C., 2017. Planktic Foraminifers in the Modern Ocean. Springer, Berlin, Heidelberg.
Schiebel, R., Waniek, J., Bork, M., Hemleben, C., 2001. Planktic foraminiferal production stimulated by chlorophyll redistribution and entrainment of nutrients. Deep-Sea Res. I Oceanogr. Res. Pap. 48 (3), 721–740. https://doi.org/10.1016/S0967-0637(00)00065-0.
Schiebel, R., Waniek, J., Zeltner, A., Alves, M., 2002. Impact of the Azores front on the distribution of planktic foraminifers, shelled gastropods, and coccolithophorids. Deep-Sea Res. II Top. Stud. Oceanogr. 49 (19), 4035–4050. https://doi.org/10.1016/S0967-0645(02)00141-8.
Schiebel, R., Zeltner, A., Treppke, U.F., Waniek, J.J., Bollmann, J., Rixen, T., Hemleben, C., 2004. Distribution of diatoms, coccolithophores and planktic foraminifers along a trophic gradient during SW monsoon in the Arabian Sea. Mar. Micropaleontol. 51 (3–4), 345–371. https://doi.org/10.1016/j.marmicro.2004.02.001.
Schiebel, R., Smart, S.M., Jentzen, A., Jonkers, L., Morard, R., Meilland, J., Haug, G.H., 2018. Advances in planktonic foraminifer research: new perspectives for paleoceanography. Rev. Micropaleontol. 61 (3), 113–138. https://doi.org/10.1016/j.revmic.2018.10.001.
Schirrmacher, J., Weinelt, M., Blanz, T., Andersen, N., Salgueiro, E., Schneider, R.R., 2019. Multi-decadal atmospheric and marine climate variability in southern Iberia during the mid-to late-Holocene. Clim. Past 15 (2), 617–634. https://doi.org/10.5194/cp-15-617-2019.
Schlesinger, M.E., Ramankutty, N., 1994. An oscillation in the global climate system of period 65–70 years. Nature 367 (6465), 723–726. https://doi.org/10.1038/367723a0.
Schlitzer, R., 2019. Ocean Data View. Retrieved from. https://odv.awi.de.
Schmidt, D.N., Renaud, S., Bollmann, J., Schiebel, R., Thierstein, H.R., 2004. Size distribution of Holocene planktic foraminifer assemblages: biogeography, ecology and adaptation. Mar. Micropaleontol. 50 (3–4), 319–338. https://doi.org/10.1016/S0377-8398(03)00098-7.
Schneider, A., Wallace, D.W., Körtzinger, A., 2007. Alkalinity of the Mediterranean sea. Geophys. Res. Lett. 34 (15) https://doi.org/10.1029/2006GL028842.
Schroeder, K., Taillandier, V., Vetrano, A., Gasparini, G.P., 2008. The circulation of the western Mediterranean Sea in spring 2005 as inferred from observations and from model outputs. Deep-Sea Res. I Oceanogr. Res. Pap. 55 (8), 947–965. https://doi.org/10.1016/j.dsr.2008.04.003.
Schroeder, K., Garcìa-Lafuente, J., Josey, S.A., Artale, V., Nardelli, B.B., Carrillo, A., Zodiatis, G., 2012. 3 - Circulation of the Mediterranean Sea and its variability. In: Lionello, P. (Ed.), The Climate of the Mediterranean Region. Elsevier, Oxford, pp. 187–256.
Shaltout, M., Omstedt, A., 2014. Recent sea surface temperature trends and future scenarios for the Mediterranean Sea. Oceanologia 56 (3), 411–443. https://doi.org/10.5697/oc.56-3.411.
Siani, G., Paterne, M., Arnold, M., Bard, E., Métivier, B., Tisnerat, N., Bassinot, F., 2000. Radiocarbon reservoir ages in the Mediterranean Sea and Black Sea. Radiocarbon 42 (2), 271–280. https://doi.org/10.1017/S0033822200059075.
Sicre, M.-A., Jalali, B., Martrat, B., Schmidt, S., Bassetti, M.-A., Kallel, N., 2016. Sea surface temperature variability in the North Western Mediterranean Sea (Gulf of Lion) during the Common Era. Earth Planet. Sci. Lett. 456, 124–133. https://doi.org/10.1016/j.epsl.2016.09.032.
Skliris, N., Sofianos, S., Gkanasos, A., Mantziafou, A., Vervatis, V., Axaopoulos, P., Lascaratos, A., 2012. Decadal scale variability of sea surface temperature in the Mediterranean Sea in relation to atmospheric variability. Ocean Dyn. 62 (1), 13–30. https://doi.org/10.1007/s10236-011-0493-5.
Smith, A.C., Wynn, P.M., Barker, P.A., Leng, M.J., Noble, S.R., Tych, W., 2016. North Atlantic forcing of moisture delivery to Europe throughout the Holocene. Sci. Rep. 6 (1), 24745. https://doi.org/10.1038/srep24745.
Smith, R.O., Bryden, H.L., Stansfield, K., 2008. Observations of new western Mediterranean deep water formation using Argo floats 2004-2006. Ocean Sci. 4 (2), 133–149. https://doi.org/10.5194/os-4-133-2008.
Sprovieri, R., Di Stefano, E., Incarbona, A., Gargano, M.E., 2003. A high-resolution record of the last deglaciation in the Sicily Channel based on foraminifera and

calcareous nannofossil quantitative distribution. Palaeogeogr. Palaeoclimatol. Palaeoecol. 202 (1), 119–142. https://doi.org/10.1016/S0031-0182(03)00632-1.
Stambler, N., 2014. The Mediterranean Sea – Primary productivity. In: Goffredo, S., Dubinsky, Z. (Eds.), The Mediterranean Sea. Its history and present challenges. Springer, Dordrecht Heidelberg New York London, pp. 113–121.
Steinhilber, F., Beer, J., Fröhlich, C., 2009. Total solar irradiance during the Holocene. Geophys. Res. Lett. 36 (19) https://doi.org/10.1029/2009GL040142.
Steinhilber, F., Abreu, J.A., Beer, J., Brunner, I., Christl, M., Fischer, H., McCracken, K.G., 2012. 9,400 years of cosmic radiation and solar activity from ice cores and tree rings. Proc. Natl. Acad. Sci. 109 (16), 5967–5971. https://doi.org/10.1073/pnas.1118965109.
Stoll, H.M., Arevalos, A., Burke, A., Ziveri, P., Mortyn, G., Shimizu, N., Unger, D., 2007. Seasonal cycles in biogenic production and export in Northern Bay of Bengal sediment traps. Deep-Sea Res. II Top. Stud. Oceanogr. 54 (5), 558–580. https://doi.org/10.1016/j.dsr2.2007.01.002.
Storz, D., Schulz, H., Waniek, J.J., Schulz-Bull, D.E., Kučera, M., 2009. Seasonal and interannual variability of the planktic foraminiferal flux in the vicinity of the Azores Current. Deep-Sea Res. I Oceanogr. Res. Pap. 56 (1), 107–124. https://doi.org/10.1016/j.dsr.2008.08.009.
Struglia, M.V., Mariotti, A., Filograsso, A., 2004. River discharge into the Mediterranean Sea: climatology and aspects of the observed variability. J. Clim. 17 (24), 4740–4751. https://doi.org/10.1175/JCLI-3225.1.
Tanhua, T., Hainbucher, D., Schroeder, K., Cardin, V., Álvarez, M., Civitarese, G., 2013. The Mediterranean Sea system: a review and an introduction to the special issue. Ocean Sci. 9, 789–803. https://doi.org/10.5194/os-9-789-2013.
Tans, P., Keeling, R.F., 2020. Trends in Atmospheric Carbon Dioxide. Retrieved from. https://www.esrl.noaa.gov/gmd/ccgg/trends/data.html.
Thiede, J., 1975. Distribution of foraminifera in surface waters of a coastal upwelling area. Nature 253 (5494), 712–714. https://doi.org/10.1038/253712a0.
Thunell, R.C., 1978. Distribution of recent planktonic foraminifera in surface sediments of the Mediterranean Sea. Mar. Micropaleontol. 3 (2), 147–173. https://doi.org/10.1016/0377-8398(78)90003-8.
Trouet, V., Esper, J., Graham, N.E., Baker, A., Scourse, J.D., Frank, D.C., 2009. Persistent positive North Atlantic Oscillation mode dominated the medieval climate anomaly. Science 324 (5923), 78–80. https://doi.org/10.1126/science.1166349.
Tsimplis, M.N., Calafat, F.M., Marcos, M., Jordá, G., Gomis, D., Fenoglio-Marc, L., Chambers, D.P., 2013. The effect of the NAO on sea level and on mass changes in the Mediterranean Sea. J. Geophys. Res. Oceans 118 (2), 944–952. https://doi.org/10.1002/jgrc.20078.
Ulbrich, U., Lionello, P., Belusic, D., Jacobeit, J., Knippertz, P., Kuglitsch, F.G., Ziv, B., 2012. 5 - Climate of the Mediterranean: Synoptic patterns, temperature, precipitation, winds and their extremes. In: Lionello, P. (Ed.), The Climate of the Mediterranean Region. Elsevier, Oxford, pp. 301–346.
Usoskin, I., Gallet, Y., Lopes, F., Kovaltsov, G., Hulot, G., 2016. Solar activity during the Holocene: the Hallstatt cycle and its consequence for grand minima and maxima. Astron. Astrophys. 587, A150. https://doi.org/10.1051/0004-6361/201527295.
Vallefuoco, M., Lirer, F., Ferraro, L., Pelosi, N., Capotondi, L., Sprovieri, M., Incarbona, A., 2012. Climatic variability and anthropogenic signatures in the Gulf of Salerno (southern-eastern Tyrrhenian Sea) during the last half millennium. Rendiconti Lincei 23 (1), 13–23. https://doi.org/10.1007/s12210-011-0154-0.
Vargas-Yáñez, M., Plaza, F., García-Lafuente, J., Sarhan, T., Vargas, J.M., Vélez-Belchi, P., 2002. About the seasonal variability of the Alboran Sea circulation. J. Mar. Syst. 35 (3), 229–248. https://doi.org/10.1016/S0924-7963(02)00128-8.
Vargas-Yáñez, M., García, M.J., Salat, J., García-Martínez, M., Pascual, J., Moya, F., 2008. Warming trends and decadal variability in the Western Mediterranean shelf. Glob. Planet. Chang. 63 (2–3), 177–184. https://doi.org/10.1016/j.gloplacha.2007.09.001.
Vargas-Yáñez, M., Moya, F., García-Martínez, M.C., Tel, E., Zunino, P., Plaza, F., Serra, M., 2010. Climate change in the Western Mediterranean Sea 1900–2008. J. Mar. Syst. 82 (3), 171–176. https://doi.org/10.1016/j.jmarsys.2010.04.013.
Vignudelli, S., Gasparini, G., Astraldi, M., Schiano, M., 1999. A possible influence of the North Atlantic Oscillation on the circulation of the Western Mediterranean Sea. Geophys. Res. Lett. 26 (5), 623–626. https://doi.org/10.1029/1999GL900038.
Volkman, J.K., Barrerr, S.M., Blackburn, S.I., Sikes, E.L., 1995. Alkenones in Gephyrocapsa oceanica: implications for studies of paleoclimate. Geochim. Cosmochim. Acta 59 (3), 513–520. https://doi.org/10.1016/0016-7037(95)00325-T.
von Schuckmann, K., Le Traon, P.-Y., Smith, N., Pascual, A., Djavidnia, S., Gattuso, J.-P., Fanjul, E.Á., 2020. Copernicus Marine Service Ocean state report, issue 4. J. Operation. Oceanogr. 13 (sup1), S1–S172. https://doi.org/10.1080/1755876X.2020.1785097.
Waelbroeck, C., Duplessy, J.-C., Michel, E., Labeyrie, L., Paillard, D., Duprat, J., 2001. The timing of the last deglaciation in North Atlantic climate records. Nature 412 (6848), 724–727. https://doi.org/10.1038/35089060.
Wang, J., Yang, B., Ljungqvist, F.C., Luterbacher, J., Osborn, Timothy J., Briffa, K.R., Zorita, E., 2017. Internal and external forcing of multidecadal Atlantic climate variability over the past 1,200 years. Nat. Geosci. 10 (7), 512–517. https://doi.org/10.1038/ngeo2962.
Wang, L., 2000. Isotopic signals in two morphotypes of Globigerinoides ruber (white) from the South China Sea: implications for monsoon climate change during the last glacial cycle. Palaeogeogr. Palaeoclimatol. Palaeoecol. 161 (3-4), 381–394. https://doi.org/10.1016/S0031-0182(00)00094-8.
Young, J.R., 1994. Functions of coccoliths. In: Winter, A., Siesser, W.G. (Eds.), Coccolithophores. Cambridge Univ. Press, pp. 63–82.
Young, J.R., Geisen, M., Cros, L., Kleijne, A., Sprengel, C., Probert, I., Østergaard, J., 2003. A guide to extant coccolithophore taxonomy. J. Nannoplankt. Res. Spec. Issue 1, 1–132.
Zarkogiannis, S., Kontakiotis, G., Antonarakou, A., 2020. Recent planktonic foraminifera population and size response to Eastern Mediterranean hydrography. Rev. Micropaleontol. 69, 100450. https://doi.org/10.1016/j.revmic.2020.100450.
Ziveri, P., Baumann, K.-H., Böckel, B., Bollmann, J., Young, J.R., 2004. Biogeography of selected Holocene coccoliths in the Atlantic Ocean. In: Thierstein, H.R., Young, J.R. (Eds.), Coccolithophores: From Molecular Processes to Global Impact. Springer Berlin Heidelberg, Berlin, Heidelberg, pp. 403–428.